LBL-34512
UC-405

Lawrence Berkeley Laboratory
UNIVERSITY OF CALIFORNIA

An Optimal Constrained Linear Inverse Method for Magnetic Source Imaging

P. Hughett

September 1993

Donner Laboratory
Biology & Medicine Division

LOAN COPY
Circulates
for 4 weeks
Bldg. 50 Library.
LBL-34512
Copy 2

Prepared for the U.S. Department of Energy under Contract Number DE-AC03-76SF00098

DISCLAIMER

This document was prepared as an account of work sponsored by the United States Government. While this document is believed to contain correct information, neither the United States Government nor any agency thereof, nor the Regents of the University of California, nor any of their employees, makes any warranty, express or implied, or assumes any legal responsibility for the accuracy, completeness, or usefulness of any information, apparatus, product, or process disclosed, or represents that its use would not infringe privately owned rights. Reference herein to any specific commercial product, process, or service by its trade name, trademark, manufacturer, or otherwise, does not necessarily constitute or imply its endorsement, recommendation, or favoring by the United States Government or any agency thereof, or the Regents of the University of California. The views and opinions of authors expressed herein do not necessarily state or reflect those of the United States Government or any agency thereof or the Regents of the University of California.

LBL-34512
UC-405

An Optimal Constrained Linear Inverse Method for Magnetic Source Imaging

Paul Hughett

Department of Electrical Engineering and Computer Sciences
University of California, Berkeley

and

Life Sciences Division
Lawrence Berkeley Laboratory
University of California
One Cyclotron Road
Berkeley CA 94720

This work was supported in part by a gift from the Advanced Technology Systems Division of the General Electric Company and in part by the Director, Office of Energy Research, Office of Health and Environmental Research, Medical Applications and Biophysical Research Division of the Department of Energy under Contract No. DE-AC03-76SF00098.

Abstract

Magnetic source imaging is the reconstruction of the current distribution inside an inaccessible volume from magnetic field measurements made outside the volume. If the unknown current distribution is expressed as a linear combination of elementary current distributions in fixed positions, then the magnetic field measurements are linear in the unknown source amplitudes and both the least square and minimum mean square reconstructions are linear problems. This offers several advantages: The problem is well understood theoretically and there is only a single, global minimum. Efficient and reliable software for numerical linear algebra is readily available.

If the sources are localized and statistically uncorrelated, then a map of expected power dissipation is equivalent to the source covariance matrix. Prior geological or physiological knowledge can be used to determine such an expected power map and thus the source covariance matrix.

The optimal constrained linear inverse method (OCLIM) derived in this paper uses this prior knowledge to obtain a minimum mean square error estimate of the current distribution. OCLIM can be efficiently computed using the Cholesky decomposition, taking about a second on a workstation-class computer for a problem with 64 sources and 144 detectors. Any source and detector configuration is allowed as long as their positions are fixed a priori. Correlations among source and noise amplitudes are permitted.

OCLIM reduces to the optimally weighted pseudoinverse method of Shim and Cho if the source amplitudes are independent and identically distributed and to the minimum-norm least squares estimate in the limit of no measurement noise or no prior knowledge of the source amplitudes. In the general case, OCLIM has better mean square error than either previous method.

OCLIM appears well suited to magnetic imaging, since it exploits prior information, provides the minimum reconstruction error, and is inexpensive to compute.

Summary of Symbols Used

$\mathbf{A}$	$= \mathsf{E}\,\mathbf{q}\mathbf{q}^T$. The a priori covariance matrix of the source amplitudes.
$\hat{\mathbf{A}}$	$= \mathsf{E}(\hat{\mathbf{q}} - \mathsf{E}\,\hat{\mathbf{q}})(\hat{\mathbf{q}} - \mathsf{E}\,\hat{\mathbf{q}})^T$. The a posteriori covariance matrix of the source amplitudes.
a_k	$= \mathbf{v}_k^T\mathbf{q}$. The component of $\mathbf{q}$ in the direction of the kth right singular vector of $\mathbf{F}$.
α_{ij}^2	$= \mathsf{E}\,q_i q_j$. The a priori cross-covariance of source amplitudes q_i and q_j. The (i,j)th entry of $\mathbf{A}$.
$\hat{\alpha}_{ij}^2$	$= \mathsf{E}\,\hat{q}_i\hat{q}_j$. The a posteriori cross-covariance of the estimated source amplitudes $\hat{q}_i$ and $\hat{q}_j$. The (i,j)th entry of $\hat{\mathbf{A}}$.
α_k^2	$= \mathsf{E}\,a_k^2 = \mathsf{E}\,\lVert\mathbf{v}_k^T\mathbf{q}\rVert^2$. The variance of a_k.
$\vec{B}(\vec{r})$	Magnetic field as a function of position.
$\vec{B}_n(\vec{r})$	Magnetic field due to the nth source.
b_m	Magnetic field measurement (including noise) at the mth detector.
$\mathbf{b}$	The vector of field measurements b_m.
$\mathbf{B}$	$= \mathsf{E}\,\mathbf{b}\mathbf{b}^T = \mathbf{F}\mathbf{A}\mathbf{F}^T + \mathbf{F}\boldsymbol{\Gamma} + \boldsymbol{\Gamma}^T\mathbf{F}^T + \boldsymbol{\Sigma}$. The covariance of the measurement vector $\mathbf{b}$.
c_k	The kth weighting coefficient in the weighted pseudoinverse.
χ^2	$= (\mathbf{b} - \mathbf{F}\hat{\mathbf{q}})^T\boldsymbol{\Sigma}^{-1}(\mathbf{b} - \mathbf{F}\hat{\mathbf{q}})$. The residual difference between the measured and reconstructed magnetic fields.
E	Expectation of a random variable or a random vector.
$\mathbf{e}$	$= \hat{\mathbf{q}} - \mathbf{q}$. The difference between the true and reconstructed current distributions.
e^2	$= \lVert\mathbf{e}\rVert^2 = \lVert\hat{\mathbf{q}} - \mathbf{q}\rVert^2$. The reconstruction error, defined as the squared difference between the true and reconstructed current distributions.
η^2	$= \mathsf{E}\,\lVert\mathbf{e}\rVert^2 = \mathsf{E}\,\lVert\hat{\mathbf{q}} - \mathbf{q}\rVert^2$. The mean reconstruction error.
F_{mn}	$= \partial b_m/\partial q_n$. Coefficient relating the field measurement b_m to the source amplitude q_n.
$\mathbf{F}$	The matrix with entries $F_{mn} = \partial b_m/\partial q_n$ relating the field measurement vector $\mathbf{b}$ to the source amplitude vector $\mathbf{q}$.

$\mathbf{F}^\dagger$	The Moore-Penrose inverse of $\mathbf{F}$.
$\mathbf{\Gamma}$	The cross-covariance of the source amplitude vector $\mathbf{q}$ and noise amplitude vector $\mathbf{w}$. Its entries are $\gamma_{ij} = \mathsf{E}\, q_i w_j$.
γ_{ij}	$= \mathsf{E}\, q_i w_j$. The covariance of the source amplitude q_i and the noise amplitude w_j.
γ_k	$= \mathsf{E}\, a_k s_k$. The covariance of a_k and s_k.
$\mathbf{H}$	A matrix representing a linear estimator of $\mathbf{q}$.
$\vec{J}(\vec{r})$	Current density as a function of position.
$\vec{J}_n(\vec{r})$	Current density contributed by the nth source.
K	Rank of $\mathbf{F}$.
K'	The lesser of M and N; the maximum possible rank of $\mathbf{F}$.
k	Index over the singular vectors of $\mathbf{F}$.
$\mathbf{L}$	$\mathbf{L}\mathbf{L}^T$ is the Cholesky decomposition of $\mathbf{B}$.
λ_k	The kth singular value of $\mathbf{F}$.
M	Total number of detectors used.
m	Index over detectors.
μ_0	Magnetic permeability of vacuum.
N	Total number of current sources in model.
n	Index over the current sources.
$\vec{p}$	Position.
q_n	Amplitude of the nth source.
$\mathbf{q}$	The vector of source amplitudes q_n.
$\hat{\mathbf{q}}$	$= \mathbf{H}\mathbf{b}$. An estimate of the source amplitude vector $\mathbf{q}$.
$\rho(\vec{r})$	Resistivity as a function of position.
ρ^2	$= \hat{\mathbf{q}}^T \mathbf{A}^{-1} \hat{\mathbf{q}}$. Surprise, defined as the goodness of fit between the reconstruction and the priors.
$\vec{r}$	Position.

$\vec{r}_m$	Position of the mth detector.
$\mathbf{R}$	$\mathbf{R}\mathbf{R}^T$ is the Cholesky decomposition of $\mathbf{A}$.
$\vec{s}_m$	Unit vector in direction of the field component sampled by the mth detector.
$\mathbf{S}$	$\mathbf{S}\mathbf{S}^T$ is the Cholesky decomposition of $\mathbf{\Sigma}$.
s_k	$= \mathbf{u}_k^T\mathbf{w}$. The component of $\mathbf{w}$ in the direction of the kth left singular vector of $\mathbf{F}$.
$\mathbf{\Sigma}$	$= \mathsf{E}\,\mathbf{w}\mathbf{w}^T$. The covariance matrix of the noise amplitude vector $\mathbf{w}$.
σ_{ij}^2	$= \mathsf{E}\,w_i w_j$. The covariance of noise amplitudes w_i and w_j. The (i,j)th entry of $\mathbf{\Sigma}$.
σ_k^2	$= \mathsf{E}\,s_k^2$. The variance of s_k.
$\mathbf{u}_k$	The kth left singular vector of $\mathbf{F}$.
$\mathbf{v}_k$	The kth right sigular vector of $\mathbf{F}$.
w_m	Noise amplitude in the mth detector.

Background

The central goal of magnetic source imaging is to reconstruct the current distribution inside some inaccessible volume from magnetic field measurements made outside that volume. It is an example of an inverse problem, as opposed to the forward problem of determining the magnetic field measurements from a known current distribution. The applications of magnetic source imaging include functional imaging of the brain and heart [1, 2, 3, 4, 5], and geophysical imaging [6, 7].

A variety of reconstruction algorithms have been used for this problem. One approach is to model the unknown current distribution as one or more current dipoles with unknown position, orientation, and magnitude and then to find the unknown parameters by a least squares fit to the observed measurements [8]. This method is computationally expensive because it is nonlinear in the unknowns and iterative solution is required. Worse, the method is often numerically unstable for two or more dipoles. Singh et al. [9] have superimposed such dipole solutions on magnetic resonance images, allowing the user to relate dipole locations to anatomic features.

A more recent approach models the unknown distribution as an array of dipoles with fixed positions but unknown magnitudes [10, 11, 12, 13, 14]. Then the magnetic field measurements $\mathbf{b}$ can be written as a linear function $\mathbf{b} = \mathbf{F}\mathbf{q} + \mathbf{w}$ of the unknown current distribution $\mathbf{q}$ and measurement noise $\mathbf{w}$. The response matrix $\mathbf{F}$ is determined by solving the forward problem for unit sources. The inverse problem in this form can be solved directly, without iteration.

The reconstruction problem of emission tomography can be written in the same linear form; the unknown distribution is radionuclide concentration. Emission tomography and magnetic source imaging both provide functional information (tracer concentration or neural activity) but the resolution and accuracy are limited by the poor signal-to-noise ratio.

Transmission tomography and magnetic resonance imaging have higher resolution but generally provide anatomic rather than functional images.

A major theme of this paper is the use of prior information, obtained by anatomic imaging or other methods, to improve the resolution and accuracy of functional imaging by constraining the set of possible solutions.

At minimum, prior knowledge must define the possible spatial locations of the sources and the locations of the detectors. This provides sufficient information to solve the forward problem and define the matrix $\mathbf{F}$. Given only this much prior information, the natural method for the inverse problem is the least-squares or minimun-norm least-squares (MNLS) method [12, 13]. This method (also known as Moore-Penrose inverse or pseudoinverse method) finds the current distribution that minimizes the squared difference between the measured fields and the fields generated by the reconstructed current distribution.

If the statistics of the measurement noise are available, maximum-likelihood (ML) methods are appropriate [15]. These methods maximize the likelihood of obtaining the measured fields given the reconstructed current distribution; if the noise is jointly Gaussian, they also minimize the squared difference between the measured and reconstructed fields, weighted to reflect the a priori noise variance.

If prior anatomical information is available from transmission tomography or magnetic resonance imaging, then it may be possible to define the a priori source variance as a function of position. Then minimum mean-square error (MMSE) methods are appropriate; they minimize the mean (average) squared difference between the true and reconstructed current distributions. Shim and Cho [16] have developed methods using a weighted pseudoinverse but their methods are optimal and useful only when the a priori source variance is constant. Helstrom [17] has developed and applied an MMSE method for image restoration; Smith et al. [18] have developed and tested an MMSE method for magnetic source imaging with general a priori source variances.

The present paper presents a unified development of the MNLS, ML, weighted pseudoinverse, and MMSE methods and shows that the weighted pseudoinverse, maximum likelihood, and MNLS methods can all be obtained as special cases of the MMSE method by an appropriate choice of priors. Formulas for the mean reconstruction error, mean residual, and a posteriori variance (or confidence limits) are derived. The paper also discusses efficient computer algorithms for the MMSE method and presents simulation results.

Oh et al. [19] have taken a different approach to the use of prior information by using the method of alternating projections to obtain "line-like" or filamentary reconstructions consistent with the measurements.

Most of the examples in this paper are taken from magnetoencephalography, but the methods should apply to magnetocardiography and geophysics as well. Furthermore, the methods should generalize to other reconstruction problems including positron emission tomography (PET) and single photon emission computed tomography (SPECT).

An Approach to the Problem

The choice of the mathematical model used to represent the prior knowledge is a compromise between several desiderata: First, the model should lead to an analytical or numerical solution method for the inverse problem; second, the parameters of the model should be physically meaningful, so that the user has some intuition of their meaning; third, the required parameters should be directly measureable (at least in principle) by some calibration experiment; fourth, the method should involve an objective criterion for correctness or optimality; and fifth, the solution method should admit some statistical test of goodness of fit between the model found and the measurements made. This paper considers one particular model that satisfies these requirements.

It is useful to exploit the fact that the magnetic field is a linear function of the current distribution. That is, the field due to a weighted sum of current sources is equal to the same weighted sum of the fields due to the individual sources. Thus, it is convenient to represent

the unknown current distribution as a weighted sum of elementary sources. The sources are chosen in advance to reflect a priori knowledge as to the location and orientation of the source currents; the weights are to be found by the inverse computation. If there is some prior information as to the magnitude of each source, it can be expressed as a probability distribution on the corresponding weight. As we will see, the prior information can also be expressed as a map of expected power density.

For example, in magnetoencephalography a set of current dipoles may be chosen as the elementary sources. The position and orientation of these dipoles are chosen to match the anatomy determined by magnetic resonance imaging. The volume currents induced by these dipoles may be included or ignored in computing the magnetic field due to each dipole.

More generally, a detailed electromagnetic finite element model [20, 21] of the brain and head could be used, choosing as the elementary sources a dipole current in each element that might contribute to the field. The volume currents are computed with the finite element model, as are the magnetic fields due to the elementary source and volume currents.

The measurements of the generated magnetic field will not be exact but will contain some measurement noise. We will assume that this noise has mean zero and that its covariance matrix is known.

Thus the prior knowledge used to constrain the reconstruction is expressed as (1) a set of elementary current sources which are consistent with the known anatomy and physiology (or geology); (2) a probability distribution for the source amplitudes; and (3) a probability distribution for the detector noise.

This approach provides both strong and weak constraints on the sources. The strong constraint is that the reconstruction will use only the selected set of elementary sources. The weak constraint is that the reconstruction will put most of the power into the more probable sources, unless the measurements clearly indicate that a less probable source is responsible. That is, a strong constraint will never be violated by the reconstruction, but a weak constraint will be, if the data support the violation.

The remainder of this paper divides roughly into three parts. The first part defines the source model and prior information and shows how to solve the forward problem of determining the field measurements from the source amplitudes. The second part defines several criteria for choosing the "best" approximate reconstruction for given measurments, derives the reconstruction methods corresponding to the different criteria, and investigates the relationships between the methods. The last part of the paper discusses the computer implementation of the methods and includes the results from a Monte Carlo simulation study.

Source Model

We choose to model the unknown current distribution $\vec{J}(\vec{r})$ as a weighted sum of N known

elementary sources $\vec{J}_n(\vec{r})$ to obtain

$$\vec{J}(\vec{r}) = \sum_{n=1}^{N} q_n \, \vec{J}_n(\vec{r}) \quad . \tag{1}$$

Each elementary source $\vec{J}_n(\vec{r})$ is a vector-valued function giving the vector current density at any position $\vec{r}$. Note that the sources are at positions fixed a priori; their positions are not free parameters to be estimated. Only the source amplitudes are unknown and must be estimated.

There are many possibilities for the set of elementary sources $\vec{J}_n(\vec{r})$, depending on the assumptions made about the unknown distribution $\vec{J}(\vec{r})$.

If the unknown distribution is assumed to be well-described by a few localized sources, then it is reasonable to use a few current dipoles whose positions, magnitudes, and orientations are to be determined. The magnetic field measurements are nonlinear functions of the source positions and iterative solution is generally necessary. The methods described in this paper assume positions fixed a priori and are not directly useful; they could possibly be used to find optimal source amplitudes at each step of an iterative scheme for improving the source position estimates. If, however, the source locations are known a priori and only the amplitudes are unknown, then the methods of this paper would be applicable.

If the unknown distribution is assumed to be smooth, then it is reasonable to expand it in a set of basis functions; these basis functions are the elementary current sources. A grid of current dipoles or a finite element mesh [20, 21] define localized elementary sources; lead fields [12], multipole expansions [22], or Fourier basis functions define non-localized elementary sources. Provided that the sources have fixed positions, the magnetic field measurements are linear functions of the source amplitudes and the linear methods developed in this paper can be used to solve the inverse problem. Any of the above basis functions could be used, though this paper considers only current dipoles in detail.

The vector $\mathbf{q}$ of source amplitudes q_n is assumed to be a random vector with mean zero and covariance matrix $\mathbf{A} = \mathsf{E}\, \mathbf{q}\mathbf{q}^T$ with entries $\alpha_{ij}^2 = \mathsf{E}\, q_i q_j$. If the expected amplitudes are not zero-mean, the shifted vector $\tilde{\mathbf{q}} = \mathbf{q} - \mathsf{E}\, \mathbf{q}$ is zero-mean and can be used instead. Since $\mathbf{A}$ is a covariance matrix, it is symmetric and positive semidefinite.

Suppose that $\rho(\vec{r})$ is the resistivity as a function of position $\vec{r}$. If we normalize each source such that

$$\int_{R^3} \rho(\vec{r}) \, |\vec{J}_n(\vec{r})|^2 \, d^3\vec{r} = 1 \quad , \tag{2}$$

then the expected (or average) power dissipation of the nth source $q_n \, \vec{J}_n$ is

$$\begin{aligned} P_n &= \mathsf{E} \int_{R^3} \rho(\vec{r}) |q_n \, \vec{J}_n(\vec{r})|^2 \, d^3\vec{r} \\ &= (\mathsf{E}\, q_n^2) \int_{R^3} \rho(\vec{r}) |\vec{J}_n(\vec{r})|^2 \, d^3\vec{r} \\ &= \alpha_{nn}^2 \quad . \end{aligned} \tag{3}$$

Thus each diagonal entry α_{nn}^2 of $\mathbf{A}$ is the expected power dissipation of the nth source acting alone.

The Forward Problem

Using the Biot-Savart Law [23], the magnetic field due to $\vec{J}$ is

$$\begin{aligned}\vec{B}(\vec{r}) &= \frac{\mu_0}{4\pi}\int_{R^3}\frac{\vec{J}(\vec{p})\times(\vec{r}-\vec{p})}{\|\vec{r}-\vec{p}\|^3}\,d^3\vec{p}\\ &= \sum_n q_n\left[\frac{\mu_0}{4\pi}\int_{R^3}\frac{\vec{J}_n(\vec{p})\times(\vec{r}-\vec{p})}{\|\vec{r}-\vec{p}\|^3}\,d^3\vec{p}\right]\\ &= \sum_n q_n\vec{B}_n(\vec{r})\end{aligned} \tag{4}$$

where

$$\vec{B}_n(\vec{r}) = \frac{\mu_0}{4\pi}\int_{R^3}\frac{\vec{J}_n(\vec{p})\times(\vec{r}-\vec{p})}{\|\vec{r}-\vec{p}\|^3}\,d^3\vec{p} \tag{5}$$

is the magnetic field at position $\vec{r}$ due to the nth source. It is assumed that the permeability is constant and equal to the permeability of vacuum $\mu_0 = 4\pi \times 10^{-7}$ H/m.

Now suppose that there are M detectors, the mth of which measures the component of the field in direction $\vec{s}_m$ at position $\vec{r}_m$. Furthermore, the measurement is contaminated by some noise w_m. Then that measurement b_m can be written as

$$\begin{aligned}b_m &= \vec{s}_m\cdot\vec{B}(\vec{r}_m) + w_m\\ &= \sum_n q_n\,\vec{s}_m\cdot\vec{B}_n(\vec{r}_m) + w_m\\ &= \sum_n q_n\left[\frac{\mu_0}{4\pi}\int_{R^3}\frac{\vec{s}_m\cdot J_n(\vec{p})\times(\vec{r}_m-\vec{p})}{\|\vec{r}_m-\vec{p}\|^3}\,d^3\vec{p}\right] + w_m\\ &= \sum_n F_{mn}\,q_n + w_m\end{aligned} \tag{6}$$

where

$$F_{mn} = \frac{\partial b_m}{\partial q_n} = \frac{\mu_0}{4\pi}\int_{R^3}\frac{\vec{s}_m\cdot J_n(\vec{p})\times(\vec{r}_m-\vec{p})}{\|\vec{r}_m-\vec{p}\|^3}\,d^3\vec{p} \tag{7}$$

is the response of the mth detector to the nth source. The response F_{mn} can also be regarded as the lead field of the mth detector integrated over the current distribution of the nth source.

Rewriting these equations for b_m in matrix form yields

$$\mathbf{b} = \mathbf{F}\mathbf{q} + \mathbf{w} \quad . \tag{8}$$

The noise vector $\mathbf{w}$ is assumed to be a random vector with mean zero and covariance matrix $\mathbf{\Sigma} = \mathsf{E}\,\mathbf{w}\mathbf{w}^T$ with entries $\sigma_{ij}^2 = \mathsf{E}\,w_i w_j$. Each diagonal entry σ_{mm}^2 is the expected

noise power of the mth detector. Since $\mathbf{\Sigma}$ is a covariance matrix, it is symmetric and positive semidefinite. If the noise is uncorrelated between sensors, then $\mathbf{\Sigma}$ is diagonal.

The cross-covariance between the source and noise amplitude vectors is $\mathbf{\Gamma} = \mathsf{E}\ \mathbf{q}\mathbf{w}^T$ with entries $\gamma_{nm} = \mathsf{E}\ q_n w_m$. In many applications, there will be no source-noise correlation and $\mathbf{\Gamma}$ will be zero.

Given these definitions, the measurement covariance is

$$\mathbf{B} = \mathsf{E}\,\mathbf{b}\mathbf{b}^T = \mathbf{F}\mathbf{A}\mathbf{F}^T + \mathbf{F}\mathbf{\Gamma} + \mathbf{\Gamma}^T\mathbf{F}^T + \mathbf{\Sigma} \quad . \tag{9}$$

In the case that $\mathbf{\Gamma} = 0$, this simplifies to $\mathbf{B} = \mathbf{F}\mathbf{A}\mathbf{F}^T + \mathbf{\Sigma}$ in which $\mathbf{F}\mathbf{A}\mathbf{F}^T$ is the variance (or power) due to the sources and $\mathbf{\Sigma}$ is the variance due to the noise. Thus we may define the signal-to-noise ratio as

$$SNR = \frac{\mathrm{Tr}(\mathbf{F}\mathbf{A}\mathbf{F}^T)}{\mathrm{Tr}(\mathbf{\Sigma})} \quad . \tag{10}$$

Note that the only assumptions made about the elementary sources $\vec{J}_n$ are that the sources are fixed in position a priori and that the superposition principle of electromagnetics holds.

Dipole Sources: In the particular case that each source $\vec{J}_n$ is a current dipole with moment $\vec{q}_n$ at position $\vec{p}_n$ (and ignoring the volume currents), the field is

$$\vec{B}_n(\vec{r}) = \frac{\mu_0}{4\pi} \cdot \frac{\vec{q}_n \times (\vec{r} - \vec{p}_n)}{\|\vec{r} - \vec{p}_n\|^3} \tag{11}$$

and the response matrix has entries

$$F_{mn} = \frac{\mu_0}{4\pi} \cdot \frac{\vec{s}_m \cdot \vec{q}_n \times (\vec{r}_m - \vec{p}_n)}{\|\vec{r}_m - \vec{p}_n\|^3} \quad . \tag{12}$$

A "rotating" dipole of unknown orientation at a given position may be represented as two or three orthogonal fixed dipoles. The fixed dipoles may be oriented along the coordinate axes; normal and tangential to the cortical surface; or along the principal axes of the assumed probability density for the rotating dipole. In the last case, the fixed dipoles will be uncorrelated.

In magnetoencephalography, a dipole source will ordinarily be oriented normal to the cortical surface and the direction of of $\vec{J}_n$ may be chosen to match. If the surface is strongly curved, a normal dipole with large expected amplitude and two tangential dipoles with smaller expected amplitude may be used.

Assumption A: We pause here to introduce a technical assumption—to be called assumption A—that will useful later. Precisely stated, we will assume hereafter that that

none of the source amplitudes q_n or the noise amplitudes w_m is almost surely equal to a linear combination of the remaining source and noise amplitudes. That is, every source and noise amplitude has some non-zero residual variance even after the effect of every other source and noise amplitude has been accounted for.

Assumption A is unlikely to be an issue in practice. About the only way to violate it is to set some a priori source variance to zero or to use some field measurement twice; the problem is easily fixed by omitting the source with zero variance (since it is known a priori), choosing a nonzero variance, or omitting the redundant measurement.

The value of assumption A is mathematical; it authorizes some algebraic manipulations that would otherwise be questionable. Specifically, Appendix A derives the following consequences to be used later:

1. The covariance matrices $\mathbf{A} = \mathsf{E}\,\mathbf{q}\mathbf{q}^T$, $\mathbf{\Sigma} = \mathsf{E}\,\mathbf{w}\mathbf{w}^T$, and $\mathbf{B} = \mathsf{E}\,\mathbf{b}\mathbf{b}^T$ are all invertible, symmetric positive definite, and have Cholesky decompositions in the forms

$$\mathbf{A} = \mathbf{R}\mathbf{R}^T, \qquad \mathbf{\Sigma} = \mathbf{S}\mathbf{S}^T, \quad \text{and} \qquad \mathbf{B} = \mathbf{L}\mathbf{L}^T \tag{13}$$

where $\mathbf{R}$, $\mathbf{S}$, and $\mathbf{L}$ are all lower triangular and invertible. Furthermore, expressions of the form $\mathbf{R}^{-1}\mathbf{X}$, $\mathbf{S}^{-1}\mathbf{X}$, or $\mathbf{L}^{-1}\mathbf{X}$ can be efficiently computed by forward substitution [24, 25] without explicitly computing the matrix inverse.

2. The form $\mathsf{E}\,||\mathbf{D}\mathbf{b}||^2$ is strictly greater than zero for every non-zero matrix $\mathbf{D}$.

Special Priors

In the general case, which will be called "correlated priors," different sources have known expected power and known correlations but the covariance matrices $\mathbf{A}$, $\mathbf{\Sigma}$, and $\mathbf{\Gamma}$ have no special structure. For example, a subject reading text might be expected to have neural activity concurrently in different parts of the primary and secondary visual cortex. More generally, electrical activity in the (normal) heart is highly correlated in patterns that depend on the phase of the cardiac cycle.

There are two special cases in which the priors take special forms leading to simplified problems.

Independent Priors: In the case of "independent priors," different sources are known (or assumed) to have different expected power but are assumed to be independent; the noise amplitudes are assumed to be independent of each other and of the sources. Then the source covariance $\mathbf{A}$ and noise covariance $\mathbf{\Sigma}$ are diagonal; the cross-covariance $\mathbf{\Gamma}$ is zero. The expected total power dissipation is $\sum_n \alpha_{nn}^2 = \operatorname{Tr}\mathbf{A}$.

If in addition each source is localized to some small volume, then most of the power dissipated by that source is contained in that volume. Computing the power density by dividing the expected power by the volume and plotting as a function of position yields a map of expected power density.

Conversely, suppose that a map of expected power density can be derived from physiological principles. Then dividing this map into small regions of approximately constant power density and assigning a singleton, pair, or triplet of orthogonal dipoles to each region yields a set of dipoles to model the unknown source distribution. The orientation of the dipole triplet should be chosen to match the principal axes of the most plausible a priori distribution; if the distribution is spherical, then the orientation does not matter and may be chosen for convenience (e.g. to match the coordinate axes). The integrated power density in each region defines the total expected power or a priori variance for the corresponding triplet (or pair or singleton); if physiology does not suggest a reasonable subdivision over the members of the triplet, equal variances seem as plausible as anything else. Then the source variances taken together define the diagonal of the a priori source covariance matrix $\mathbf{A}$.

For example, sources located in the grey matter (as determined by magnetic resonance imaging) might be oriented normal to the cortex and assigned twice the expected power of sources in the white matter or cerebrospinal fluid; sources outside the head would be omitted entirely.

Uniform Priors: In the case of "uniform priors," the approximate amplitude of the elementary sources is known but there is no basis for believing that any one is more active than any other; and the same is true of the noise amplitudes. That is, the source amplitudes are independent and identically distributed; so are the noise amplitudes. Then every source has the same expected activity α^2, the covariance matrix $\mathbf{A}$ takes the form $\alpha^2\mathbf{I}$, and the map of expected activity is uniform; the noise covariance $\mathbf{\Sigma}$ takes the form $\sigma^2\mathbf{I}$ and the cross-covariance $\mathbf{\Gamma}$ is zero.

The Inverse Problem

The inverse problem is to find a "best" estimate $\hat{\mathbf{q}}$ of the unknown source amplitude vector $\mathbf{q}$ from given values for the response matrix $\mathbf{F}$, the field measurements $\mathbf{b}$, and perhaps other information such as the noise covariance $\mathbf{\Sigma}$ and the source covariance $\mathbf{A}$.

This paper considers only linear inverse methods. That is, the best estimate $\hat{\mathbf{q}}$ is always computed in the form

$$\hat{\mathbf{q}} = \mathbf{H}\mathbf{b} \tag{14}$$

where $\mathbf{H}$ is a linear operator possibly depending on $\mathbf{A}$, $\mathbf{\Sigma}$, $\mathbf{\Gamma}$, or other prior information.

The simple solution $\hat{\mathbf{q}} = \mathbf{F}^{-1}\mathbf{b}$ does not work in general for inverse problems; $\mathbf{F}$ is rarely invertible and usually rectangular. The inverse problem is often both overdetermined in the sense that no solution $\hat{\mathbf{q}}$ exactly solves $\mathbf{F}\mathbf{q} = \mathbf{b}$ and underdetermined in that many different values of $\hat{\mathbf{q}}$ provide equally close approximations. Different criteria for the "best" approximation lead to different inverse methods.

The least squares (LS) criterion [26] is to minimize the residual

$$\varepsilon^2 = ||\mathbf{b} - \mathbf{F}\hat{\mathbf{q}}||^2 \quad , \tag{15}$$

which is a measure of the discrepancy between the measured and reconstucted field values. The least squares solution is not necessarily unique; there may be many different solutions that achieve the minimum ε^2. The minimum-norm least squares (MNLS) criterion chooses from all these minimum-residual solutions the unique solution with smallest norm $||\hat{\mathbf{q}}||^2$. No prior information is necessary and the value of ε^2 can be computed for any given $\mathbf{b}$.

The maximum likelihood (ML) criterion [26] is, assuming that $\mathbf{w}$ is jointly Gaussian, to minimize the weighted residual

$$\chi^2 = (\mathbf{b} - \mathbf{F}\hat{\mathbf{q}})^T \mathbf{\Sigma}^{-1} (\mathbf{b} - \mathbf{F}\hat{\mathbf{q}}) \quad , \tag{16}$$

which is a measure of the discrepancy between the measured and reconstructed field values, weighted by the a priori noise variance. As with least squares, the solution is not necessarily unique. Noise statistics are required but source statistics are not.

If the noise amplitudes are assumed to be independent and identically distributed ($\mathbf{\Sigma} = \sigma^2 \mathbf{I}$), then the MNLS solution minimizes the χ^2 statistic and is also the maximum likelihood solution.

The residual χ^2 can also be evaluated in terms of the given measurements $\mathbf{b}$ for any estimator $\mathbf{H}$:

$$\begin{aligned} \chi^2 &= (\mathbf{b} - \mathbf{F}\hat{\mathbf{q}})^T \mathbf{\Sigma}^{-1} (\mathbf{b} - \mathbf{F}\hat{\mathbf{q}}) \\ &= (\mathbf{b} - \mathbf{FHb})^T \mathbf{S}^{-T} \mathbf{S}^{-1} (\mathbf{b} - \mathbf{FHb}) \\ &= ||\mathbf{S}^{-1}(\mathbf{I} - \mathbf{FH})\mathbf{b}||^2 \end{aligned} \tag{17}$$

which is a convenient form for computer implementation. The mean value $\mathsf{E}\,\chi^2$ of the residual reveals how closely a reconstruction matches the given measurements on average and is useful as a figure of merit for a reconstruction filter $\mathbf{H}$. It can be computed as

$$\begin{aligned} \mathsf{E}\,\chi^2 &= \mathsf{E}\,||\mathbf{S}^{-1}(\mathbf{I} - \mathbf{FH})\mathbf{b}||^2 \\ &= \mathrm{Tr}(\mathbf{S}^{-1}(\mathbf{I} - \mathbf{FH})\mathbf{B}(\mathbf{I} - \mathbf{FH})^T \mathbf{S}^{-T}) \\ &= \mathrm{Tr}((\mathbf{S}^{-1}(\mathbf{I} - \mathbf{FH})\mathbf{L})(\mathbf{S}^{-1}(\mathbf{I} - \mathbf{FH})\mathbf{L})^T) \\ &= ||\mathbf{S}^{-1}(\mathbf{I} - \mathbf{FH})\mathbf{L}||_F^2 \end{aligned} \tag{18}$$

where the Frobenius norm of a general matrix $\mathbf{G}$ is defined by

$$||\mathbf{G}||_F^2 = \sum_{ij} g_{ij}^2 = \mathrm{Tr}(\mathbf{G}\mathbf{G}^T) \quad .$$

The minimum mean square error (MMSE) or mean square (M.S.) criterion [27] is to minimize the average reconstruction error

$$\eta^2 = \mathsf{E}\,e^2 = \mathsf{E}\,||\hat{\mathbf{q}} - \mathbf{q}||^2 \quad , \tag{19}$$

which is a measure of the discrepancy between the reconstructed and the true current distributions. The error $e^2 = ||\hat{\mathbf{q}} - \mathbf{q}||^2$ depends on the true distribution and thus cannot

be computed for any specific $\mathbf{b}$; only its mean value η^2 can be determined. The mean square error η^2 depends on the source and noise statistics, so both of these must be known (or assumed) a priori.

For a given filter $\mathbf{H}$, the mean square error takes the form

$$\begin{aligned}\eta^2 &= \mathsf{E}\,\|\mathbf{H}(\mathbf{F}\mathbf{q}+\mathbf{w})-\mathbf{q}\|^2 \\ &= \mathsf{E}\,\|(\mathbf{HF}-\mathbf{I})\mathbf{q}\|^2 + \mathsf{E}\,\|\mathbf{H}\mathbf{w}\|^2 + 2\,\mathsf{E}(\mathbf{H}\mathbf{w})^T(\mathbf{HF}-\mathbf{I})\mathbf{q} \\ &= \mathrm{Tr}((\mathbf{HF}-\mathbf{I})\mathbf{A}(\mathbf{HF}-\mathbf{I})^T + \mathbf{H}\boldsymbol{\Sigma}\mathbf{H}^T + 2(\mathbf{HF}-\mathbf{I})\boldsymbol{\Gamma}\mathbf{H}^T) \quad . \end{aligned} \tag{20}$$

Also of interest is the function

$$\rho^2 = \hat{\mathbf{q}}^T\mathbf{A}^{-1}\hat{\mathbf{q}} \quad , \tag{21}$$

which is a measure of the goodness of fit between the reconstructed current distribution and the a priori current distribution. Since ρ^2 increases as the reconstruction becomes less likely relative to the priors, it will be called the "surprise." For given $\mathbf{b}$ and $\mathbf{H}$, it has the value

$$\begin{aligned}\rho^2 &= \hat{\mathbf{q}}^T\mathbf{A}^{-1}\hat{\mathbf{q}} \\ &= (\mathbf{b}^T\mathbf{H}^T\mathbf{R}^{-T})(\mathbf{R}^{-1}\mathbf{H}\mathbf{b}) \\ &= \|\mathbf{R}^{-1}\mathbf{H}\mathbf{b}\|^2 \quad . \end{aligned} \tag{22}$$

The mean surprise indicates to what extent the reconstruction filter uses the prior information rather than the given measurements; it has the value

$$\begin{aligned}\mathsf{E}\,\rho^2 &= \mathsf{E}\,\|\mathbf{R}^{-1}\mathbf{H}\mathbf{b}\|^2 \\ &= \mathrm{Tr}(\mathbf{R}^{-1}\mathbf{H}\mathbf{B}\mathbf{H}^T\mathbf{R}^{-T}) \\ &= \mathrm{Tr}((\mathbf{R}^{-1}\mathbf{H}\mathbf{L})(\mathbf{R}^{-1}\mathbf{H}\mathbf{L})^T) \\ &= \|(\mathbf{R}^{-1}\mathbf{H}\mathbf{L})\|_F^2 \quad . \end{aligned} \tag{23}$$

Minimum-Norm Least Squares Method

The Moore-Penrose generalized inverse (sometimes known simply as the pseudoinverse) is a generalization of the matrix inverse to arbitrary rectangular matrices. It was first reported by Moore [28] in 1920 as the unique matrix satisfying certain algebraic conditions not relevant here, and rediscovered by Penrose [29] in 1955 using different but equivalent algebraic conditions. Of importance to the present paper is the fact [30] that it computes the MNLS solution.

The Moore-Penrose inverse can be easily computed from the singular value decomposition (SVD) [24, 25] of the response matrix $\mathbf{F}$. To fix notation, the SVD theorem states that the $M \times N$ response matrix $\mathbf{F}$ can be decomposed in the form

$$\mathbf{F} = \mathbf{U}\boldsymbol{\Lambda}\mathbf{V}^T = \sum_{k=1}^{K} \lambda_k\, \mathbf{u}_k\mathbf{v}_k^T \tag{24}$$

where $K \leq K' = \min(M, N)$ is the rank of $\mathbf{F}$; $\mathbf{U}$ is an orthogonal matrix with orthonormal columns $\mathbf{u}_k$; $\mathbf{V}$ is an orthogonal matrix with orthonormal columns $\mathbf{v}_k$; and $\mathbf{\Lambda}$ is an $M \times N$ diagonal matrix with diagonal entries $\lambda_1 \geq \lambda_2 \geq \cdots \geq \lambda_K > \lambda_{K+1} = \cdots = \lambda_{K'} = 0$. The values λ_k for $k = 1, \ldots, K$ are called the singular values of $\mathbf{F}$; the vectors $\mathbf{u}_k$ and $\mathbf{v}_k$ for $k = 1, \ldots, K$ are respectively called the left and right singular vectors of $\mathbf{F}$. The additional vectors $\mathbf{u}_k, k = K+1, \ldots, M$, span the complement of the range space of $\mathbf{F}$; the additional vectors $\mathbf{v}_k, k = K+1, \ldots, N$, span the null space of $\mathbf{F}$.

The Moore-Penrose inverse of $\mathbf{F}$ is then

$$\mathbf{F}^\dagger = \sum_{\lambda_k \neq 0} \lambda_k^{-1} \mathbf{v}_k \mathbf{u}_k^T \tag{25}$$

and is equal to the ordinary matrix inverse if $\mathbf{F}$ is non-singular. If $\mathbf{F}$ is singular, the system $\mathbf{F}\mathbf{q} = \mathbf{b}$ is ill-posed and has infinitely many possible solutions $\mathbf{q}$; $\hat{\mathbf{q}} = \mathbf{F}^\dagger \mathbf{b}$ is the particular solution with the smallest norm, or the minimum-norm least squares (MNLS) solution.

The Moore-Penrose inverse in its pure form is not generally suitable for inverse problems with measurement noise. Suppose that $\mathbf{b} = \mathbf{F}\mathbf{q} + \mathbf{w}$ and consider the estimate $\hat{\mathbf{q}} = \mathbf{F}^\dagger \mathbf{b} = \mathbf{F}^\dagger \mathbf{F}\mathbf{q} + \mathbf{F}^\dagger \mathbf{w}$. The error due to noise is

$$\mathbf{F}^\dagger \mathbf{w} = \sum_{\lambda_k \neq 0} \lambda_k^{-1} (\mathbf{u}_k^T \mathbf{w}) \mathbf{v}_k \quad , \tag{26}$$

which grows without bound as the singular values λ_k decrease toward zero. The error in $\hat{\mathbf{q}}$ is roughly proportional to the reciprocal of the smallest singular value and can easily swamp the correct answer.

One simple cure is to drop all singular values less than a threshold ϵ, defining a truncated pseudoinverse

$$\mathbf{F}^\epsilon = \sum_{\lambda_k > \epsilon} \lambda_k^{-1} \mathbf{v}_k \mathbf{u}_k^T \quad . \tag{27}$$

Wang, Williamson, and Kaufman [12, 13] have used a truncated pseudoinverse for magnetic source imaging, although they do not state their truncation criterion. Choosing the threshold ϵ can be problematic; the weighted pseudoinverse method discussed below provides one systematic approach.

Weighted Pseudoinverse Methods

To avoid these numerical problems, Shim and Cho [16] have modified the MNLS by defining a weighted pseudoinverse (which they call the stochastic SVD pseudoinverse)

$$\mathbf{F}^w = \sum_{\lambda_k \neq 0} c_k \lambda_k^{-1} \mathbf{v}_k \mathbf{u}_k^T \quad , \tag{28}$$

where the weights c_k are chosen to yield the minimum mean square error. Restricting the weights to zero and one yields a truncated pseudoinverse. Their derivation and results unfortunately contain some typographical errors; the following derivation hopefully corrects

those errors without introducing any new ones, and generalizes their result by allowing correlations between noise and source amplitudes ($\mathbf{\Gamma} \neq 0$).

Shim and Cho have applied the optimal truncated pseudoinverse method (OTPIM) and optimal weighted pseudoinverse method (OWPIM) to PET reconstruction; Jeffs, Leahy, and Singh [11] have used the optimal truncated pseudoinverse for magnetic source imaging of the brain.

To determine the optimal c_k, write the source and noise vectors in terms of the singular vectors of $\mathbf{F}$ to obtain

$$\mathbf{q} = \sum_{k=1}^{N} a_k \mathbf{v}_k \qquad \text{and} \qquad \mathbf{w} = \sum_{k=1}^{M} s_k \mathbf{u}_k \quad . \tag{29}$$

Note that $a_k = \mathbf{v}_k^T \mathbf{q}$ and $s_k = \mathbf{u}_k^T \mathbf{w}$, so that $\mathsf{E}\, a_k = 0$ and $\mathsf{E}\, s_k = 0$. Define the covariances

$$\begin{aligned} \alpha_k^2 = \mathsf{E}\, a_k^2 &= \mathbf{v}_k^T \mathbf{A} \mathbf{v}_k \quad , \qquad k = 1, \ldots, N \quad ; \\ \sigma_k^2 = \mathsf{E}\, s_k^2 &= \mathbf{u}_k^T \mathbf{\Sigma} \mathbf{u}_k \quad , \qquad k = 1, \ldots, M \quad ; \text{and} \\ \gamma_k = \mathsf{E}\, a_k\, s_k &= \mathbf{v}_k^T \mathbf{\Gamma} \mathbf{u}_k \quad , \qquad k = 1, \ldots, K' \end{aligned} \tag{30}$$

which are the diagonal entries of the rotated covariance matrices $\mathbf{V}^T\mathbf{A}\mathbf{V}$, $\mathbf{U}^T\mathbf{\Sigma}\mathbf{U}$, and $\mathbf{V}^T\mathbf{\Gamma}\mathbf{U}$ respectively. The notation here may be a bit confusing; the symbols α_{ij}^2, σ_{ij}^2, and γ_{ij} with *two* subscripts denote the entries of the *unrotated* covariance matrices $\mathbf{A}$, $\mathbf{\Sigma}$, and $\mathbf{\Gamma}$.

The optimal estimate of $\mathbf{q}$ is $\hat{\mathbf{q}} = \mathbf{F}^w \mathbf{b}$ with error

$$\begin{aligned} \mathbf{e} = \hat{\mathbf{q}} - \mathbf{q} &= \mathbf{F}^w \mathbf{b} - \mathbf{q} = \mathbf{F}^w(\mathbf{F}\mathbf{q} + \mathbf{w}) - \mathbf{q} \\ &= \mathbf{F}^w \mathbf{F} \mathbf{q} - \mathbf{q} + \mathbf{F}^w \mathbf{w} \\ &= \mathbf{F}^w \mathbf{F} \sum_{k=1}^{N} a_k \mathbf{v}_k - \sum_{k=1}^{N} a_k \mathbf{v}_k + \mathbf{F}^w \sum_{k=1}^{M} s_k \mathbf{u}_k \quad ; \end{aligned}$$

and since $\mathbf{v}_{K+1}, \ldots, \mathbf{v}_N$ are in the null space of $\mathbf{F}$ and $\mathbf{u}_{K+1}, \ldots, \mathbf{u}_M$ are in the null space of $\mathbf{F}^w$,

$$\begin{aligned} \mathbf{e} &= \mathbf{F}^w \mathbf{F} \sum_{k=1}^{K} a_k \mathbf{v}_k - \sum_{k=1}^{N} a_k \mathbf{v}_k + \mathbf{F}^w \sum_{k=1}^{K} s_k \mathbf{u}_k \\ &= \sum_{k=1}^{K} \left[(c_k - 1) a_k + \frac{c_k\, s_k}{\lambda_k} \right] \mathbf{v}_k - \sum_{k=K+1}^{N} a_k \mathbf{v}_k \quad . \end{aligned} \tag{31}$$

Then the mean square error is

$$\eta^2 = \mathsf{E}\, \mathbf{e}^T \mathbf{e} = \sum_{k=1}^{K} \left[(c_k - 1)^2 \alpha_k^2 + 2 c_k (c_k - 1) \gamma_k / \lambda_k + c_k^2 \sigma_k^2 / \lambda_k^2 \right] + \sum_{k=K+1}^{N} \alpha_k^2 \quad . \tag{32}$$

Finding the minimum by the usual procedure yields the coefficients

$$c_k = \frac{\alpha_k^2 \lambda_k^2 + \gamma_k \lambda_k}{\alpha_k^2 \lambda_k^2 + 2\gamma_k \lambda_k + \sigma_k^2} \quad , \qquad k = 1, \ldots, K \tag{33}$$

for the optimal weighted pseudoinverse of $\mathbf{F}$.

Note that the off-diagonal covariances $\mathsf{E}\, a_k a_l$, $\mathsf{E}\, s_k s_l$, and $\mathsf{E}\, a_k s_l$ with $k \neq l$ do not appear in the above expression. In effect, they are assumed to be zero. Equivalently, the covariance matrices $\mathbf{V}^T\mathbf{A}\mathbf{V}$, $\mathbf{U}^T\mathbf{\Sigma}\mathbf{U}$, and $\mathbf{V}^T\mathbf{\Gamma}\mathbf{U}$ are assumed to be diagonal. This is called the case of "coaxial" priors and will be discussed later.

If the weights are restricted to $c_k = 0$ or $c_k = 1$, the weighted pseudoinverse becomes a truncated pseudoinverse. Thus, any truncated pseudoinverse is a special case of the weighted pseudoinverse and will, in general, have a larger error than the optimal weighted pseudoinverse.

To obtain the optimal truncated pseudoinverse, consider the kth error term

$$\begin{aligned} \eta_k^2 &= (c_k - 1)^2 \alpha_k^2 + 2c_k(c_k - 1)\gamma_k/\lambda_k + c_k^2 \sigma_k^2/\lambda_k^2 \\ &= \begin{cases} \alpha_k^2 & \text{if } c_k = 0 \\ \sigma_k^2/\lambda_k^2 & \text{if } c_k = 1 \end{cases} \end{aligned} \tag{34}$$

The minimum error is achieved when the smaller of the two possible values is taken; that is, the kth term should be retained if $\sigma_k^2/\lambda_k^2 < \alpha_k^2 \Leftrightarrow \lambda_k > \sigma_k/\alpha_k$ and dropped otherwise. Thus the optimal truncated pseudoinverse is

$$\mathbf{F}^t = \sum_{\lambda_k > \sigma_k/\alpha_k} \lambda_k^{-1} \mathbf{v}_k \mathbf{u}_k^T \quad . \tag{35}$$

Setting $\sigma_k^2/\lambda_k^2 = \alpha_k^2$ in equation (33) yields $c_k = \frac{1}{2}$, so rounding c_k to 0 or 1 in the optimal weighted pseudoinverse yields the optimal truncated pseudoinverse.

The figures of merit η^2, $\mathsf{E}\,\chi^2$, and $\mathsf{E}\,\rho^2$ take special forms for the weighted pseudoinverse. The reconstruction error η^2 is most easily computed using the formula (32) given above for coaxial priors or formula (20) for general priors. The mean residual is $\mathsf{E}\,\chi^2 = \|\mathbf{S}^{-1}(\mathbf{I} - \mathbf{F}\mathbf{H})\mathbf{L}\|_F^2$ where

$$\mathbf{I} - \mathbf{F}\mathbf{H} = \sum_{k=1}^{M} (1 - c_k) \mathbf{u}_k \mathbf{u}_k^T \quad . \tag{36}$$

Substituting yields

$$\mathsf{E}\,\chi^2 = \left\| \sum_{k=1}^{M} (1 - c_k)(\mathbf{S}^{-1}\mathbf{u}_k)(\mathbf{L}^T\mathbf{u}_k)^T \right\|_F^2 \quad . \tag{37}$$

The mean surprise is

$$\begin{aligned}
\mathsf{E}\,\rho^2 &= \|\mathbf{R}^{-1}\mathbf{H}\mathbf{L}\|_F^2 \\
&= \left\| \mathbf{R}^{-1} \left(\sum_{k=1}^{K} c_k \lambda_k^{-1} \mathbf{v}_k \mathbf{u}_k^T \right) \mathbf{L} \right\|_F^2 \\
&= \left\| \sum_{k=1}^{K} c_k \lambda_k^{-1} (\mathbf{R}^{-1}\mathbf{v}_k)(\mathbf{L}^T\mathbf{u}_k)^T \right\|_F^2 \quad . \qquad (38)
\end{aligned}$$

Optimal Constrained Linear Inverse Method

The Shim-Cho weighted pseudoinverse is optimal (in the MMSE sense) over all possible weighted pseudoinverses but is not, in general, optimal over all possible linear estimators of the form $\hat{\mathbf{q}} = \mathbf{H}\mathbf{b}$.

The optimal constrained linear estimator is given by the matrix $\mathbf{H}$ that minimizes

$$\begin{aligned}
\eta^2 &= \mathsf{E}\,\|\hat{\mathbf{q}} - \mathbf{q}\|^2 = \mathsf{E}\,\|\mathbf{H}\mathbf{b} - \mathbf{q}\|^2 \\
&= \mathsf{E}\,\|\mathbf{H}(\mathbf{F}\mathbf{q} + \mathbf{w}) - \mathbf{q}\|^2 \\
&= \mathsf{E}\,\|(\mathbf{H}\mathbf{F} - \mathbf{I})\mathbf{q} + \mathbf{H}\mathbf{w}\|^2 \quad . \qquad (39)
\end{aligned}$$

Now consider a variation $\mathbf{H} + \epsilon\,\delta\mathbf{H}$ where ϵ is a scalar and $\delta\mathbf{H}$ is a matrix to obtain

$$\begin{aligned}
\eta^2 &= \mathsf{E}\,\|(\mathbf{H}\mathbf{F} + \epsilon\,\delta\mathbf{H}\mathbf{F} - \mathbf{I})\mathbf{q} + \mathbf{H}\mathbf{w} + \epsilon\,\delta\mathbf{H}\mathbf{w}\|^2 \\
&= \mathsf{E}\,\|(\mathbf{H}\mathbf{F} - \mathbf{I})\mathbf{q} + \mathbf{H}\mathbf{w} + \epsilon\,\delta\mathbf{H}(\mathbf{F}\mathbf{q} + \mathbf{w})\|^2 \\
&= \mathsf{E}\,\|(\mathbf{H}\mathbf{F} - \mathbf{I})\mathbf{q} + \mathbf{H}\mathbf{w}\|^2 \\
&\qquad + 2\epsilon\ \mathsf{E}(\mathbf{F}\mathbf{q} + \mathbf{w})^T\,\delta\mathbf{H}^T[(\mathbf{H}\mathbf{F} - \mathbf{I})\mathbf{q} + \mathbf{H}\mathbf{w}] \\
&\qquad + \epsilon^2\ \mathsf{E}\,\|\delta\mathbf{H}(\mathbf{F}\mathbf{q} + \mathbf{w})\|^2 \\
&= c_0 + c_1\epsilon + c_2\epsilon^2 \qquad (40)
\end{aligned}$$

for scalars c_0, c_1, and c_2 which depend on $\delta\mathbf{H}$.

Now $\mathbf{H}$ can minimize η^2 only if c_1 is zero for any value of $\delta\mathbf{H}$. To see this, assume on the contrary that there is some non-zero $\delta\mathbf{H}$ such that c_1 is not zero. Assumption A ensures that the constant $c_2 = \mathsf{E}\,\|\delta\mathbf{H}(\mathbf{F}\mathbf{q} + \mathbf{w})\|^2$ is positive whenever $\delta\mathbf{H}$ is not zero. Then η^2 has a unique minimum at $\epsilon_{min} = -c_1/(2c_2)$. But this means that η^2 is smaller for $\mathbf{H} + \epsilon_{min}\,\delta\mathbf{H}$ than for $\mathbf{H}$. Thus, contrary to our assumption, $\mathbf{H}$ is not the minimum. Therefore, c_1 must be zero for every $\delta\mathbf{H}$.

The positivity of c_2 also guarentees that η^2 has a minimum rather than a maximum. Furthermore, since η^2 is quadratic in ϵ, the minimum is unique and there is no maximum. That is, the optimal $\mathbf{H}$ exists and is unique.

Now observe that, for random vectors $\mathbf{x}$ and $\mathbf{y}$, the expection $\mathsf{E}\,\mathbf{x}^T\mathbf{D}\mathbf{y}$ is zero for all $\mathbf{D}$ only if $\mathsf{E}\,\mathbf{x}\mathbf{y}^T = 0$. (Consider the set of matrices $\mathbf{D}$ in which one entry takes the value one and all the other entries are zero.) Then the scalar c_1 can be zero for arbitrary $\delta\mathbf{H}$ only if

$$\begin{aligned} 0 &= \mathsf{E}\,[(\mathbf{HF}-\mathbf{I})\mathbf{q}+\mathbf{Hw}](\mathbf{Fq}+\mathbf{w})^T \\ &= \mathsf{E}\,\mathbf{HFqq}^T\mathbf{F}^T - \mathsf{E}\,\mathbf{qq}^T\mathbf{F}^T + \mathsf{E}\,\mathbf{Hwq}^T\mathbf{F}^T + \mathsf{E}\,\mathbf{HFqw}^T - \mathsf{E}\,\mathbf{qw}^T + \mathsf{E}\,\mathbf{Hww}^T \\ &= \mathbf{HFAF}^T - \mathbf{AF}^T + \mathbf{H\Gamma}^T\mathbf{F}^T + \mathbf{HF\Gamma} - \mathbf{\Gamma} + \mathbf{H\Sigma} \quad , \end{aligned} \tag{41}$$

which can be solved to yield

$$\mathbf{H} = (\mathbf{AF}^T + \mathbf{\Gamma})(\mathbf{FAF}^T + \mathbf{F\Gamma} + \mathbf{\Gamma}^T\mathbf{F}^T + \mathbf{\Sigma})^{-1} \tag{42}$$

where assumption A guarentees the existence of the inverse.

The mean residual, mean square error, and mean surprise can be computed from the formulas (18), (20), and (23) given above for a generic linear estimation.

Useful Special Cases

There are several special cases in which the OCLIM filter takes simpler forms.

Noise Uncorrelated with Sources: If the noise is uncorrelated with the sources, then $\mathbf{\Gamma} = 0$ and the filter simplifies to

$$\mathbf{H} = \mathbf{AF}^T(\mathbf{FAF}^T + \mathbf{\Sigma})^{-1} \quad . \tag{43}$$

This mean square estimator has been previously used by Helstrom [17] and others [31] for image restoration and by Smith et al. [18] for magnetic source imaging.

It is also related to the backprojection of filtered projections algorithm for emission tomography [32], also called the filtered backprojection algorithm [33]. The factor $(\mathbf{FAF}^T + \mathbf{\Sigma})^{-1}$ filters the projections $\mathbf{b}$, the factor $\mathbf{F}^T$ backprojects, and $\mathbf{A}$ weights the result according to the a priori probabilities.

Furthermore, observe that

$$\begin{aligned} & \mathbf{F}^T + \mathbf{F}^T\mathbf{\Sigma}^{-1}\mathbf{FAF}^T = \mathbf{F}^T\mathbf{\Sigma}^{-1}\mathbf{FAF}^T + \mathbf{F}^T \\ \Leftrightarrow\ & (\mathbf{A}^{-1} + \mathbf{F}^T\mathbf{\Sigma}^{-1}\mathbf{F})\mathbf{AF}^T = \mathbf{F}^T\mathbf{\Sigma}^{-1}(\mathbf{FAF}^T + \mathbf{\Sigma}) \\ \Leftrightarrow\ & \mathbf{AF}^T(\mathbf{FAF}^T + \mathbf{\Sigma})^{-1} = (\mathbf{A}^{-1} + \mathbf{F}^T\mathbf{\Sigma}^{-1}\mathbf{F})^{-1}\mathbf{F}^T\mathbf{\Sigma}^{-1} \quad . \end{aligned} \tag{44}$$

Thus the optimal filter can also be written in the form

$$\mathbf{H} = (\mathbf{A}^{-1} + \mathbf{F}^T\mathbf{\Sigma}^{-1}\mathbf{F})^{-1}\mathbf{F}^T\mathbf{\Sigma}^{-1} \quad . \tag{45}$$

This form represents a variant backprojection algorithm in which filtering is done after backprojection; Budinger at al. call this the "filter of the backprojection algorithm" [32].

The factor $\mathbf{\Sigma}^{-1}$ corrects for noise variance in the projections, $\mathbf{F}^T$ backprojects, and $(\mathbf{A}^{-1}+\mathbf{F}^T\mathbf{\Sigma}^{-1}\mathbf{F})^{-1}$ filters the backprojected image.

Using the fact that

$$\begin{aligned}\mathbf{HF}-\mathbf{I} &= (\mathbf{A}^{-1}+\mathbf{F}^T\mathbf{\Sigma}^{-1}\mathbf{F})^{-1}\mathbf{F}^T\mathbf{\Sigma}^{-1}\mathbf{F}-\mathbf{I} \\ &= -(\mathbf{A}^{-1}+\mathbf{F}^T\mathbf{\Sigma}^{-1}\mathbf{F})^{-1}\mathbf{A}^{-1} \quad . \end{aligned} \tag{46}$$

and substituting into (20) yields the mean square error

$$\begin{aligned}\eta^2 &= \mathrm{Tr}((\mathbf{A}^{-1}+\mathbf{F}^T\mathbf{\Sigma}^{-1}\mathbf{F})^{-1}\mathbf{A}^{-1}\mathbf{A}\mathbf{A}^{-1}(\mathbf{A}^{-1}+\mathbf{F}^T\mathbf{\Sigma}^{-1}\mathbf{F})^{-1} \\ &\quad + (\mathbf{A}^{-1}+\mathbf{F}^T\mathbf{\Sigma}^{-1}\mathbf{F})^{-1}\mathbf{F}^T\mathbf{\Sigma}^{-1}\mathbf{\Sigma}\mathbf{\Sigma}^{-1}\mathbf{F}(\mathbf{A}^{-1}+\mathbf{F}^T\mathbf{\Sigma}^{-1}\mathbf{F})^{-1}) \\ &= \mathrm{Tr}((\mathbf{A}^{-1}+\mathbf{F}^T\mathbf{\Sigma}^{-1}\mathbf{F})^{-1}) \\ &= \mathrm{Tr}(\mathbf{A}-\mathbf{A}\mathbf{F}^T(\mathbf{F}\mathbf{A}\mathbf{F}^T+\mathbf{\Sigma})^{-1}\mathbf{F}\mathbf{A}) \\ &= \mathrm{Tr}(\mathbf{A}-(\mathbf{L}^{-1}\mathbf{F}\mathbf{A})^T(\mathbf{L}^{-1}\mathbf{F}\mathbf{A})) \\ &= \mathrm{Tr}(\mathbf{A})-\|\mathbf{L}^{-1}\mathbf{F}\mathbf{A}\|_F^2 \quad . \end{aligned} \tag{47}$$

Alternatively, η^2 can be computed from the a posteriori variance $\hat{\mathbf{A}}$ discussed later.

To find the mean residual and mean surprise, first observe that

$$\begin{aligned}\mathbf{H} &= \mathbf{A}\mathbf{F}^T(\mathbf{F}\mathbf{A}\mathbf{F}^T+\mathbf{\Sigma})^{-1} \\ &= \mathbf{R}\mathbf{R}^T\mathbf{F}^T\mathbf{L}^{-T}\mathbf{L}^{-1} \end{aligned} \tag{48}$$

and

$$\begin{aligned}\mathbf{I}-\mathbf{FH} &= \mathbf{I}-\mathbf{F}\mathbf{A}\mathbf{F}^T(\mathbf{F}\mathbf{A}\mathbf{F}^T+\mathbf{\Sigma})^{-1} \\ &= \mathbf{\Sigma}(\mathbf{F}\mathbf{A}\mathbf{F}^T+\mathbf{\Sigma})^{-1} \\ &= \mathbf{S}\mathbf{S}^T\mathbf{L}^{-T}\mathbf{L}^{-1} \quad . \end{aligned} \tag{49}$$

It then follows from (18) and (23) that

$$\mathsf{E}\,\chi^2 = \|\mathbf{S}^T\mathbf{L}^{-T}\|_F^2 = \|\mathbf{L}^{-1}\mathbf{S}\|_F^2 \tag{50}$$

and

$$\mathsf{E}\,\rho^2 = \|\mathbf{R}^T\mathbf{F}^T\mathbf{L}^{-T}\|_F^2 = \|\mathbf{L}^{-1}\mathbf{F}\mathbf{R}\|_F^2 \quad . \tag{51}$$

Coaxial priors: Suppose that the covariance matrices $\mathbf{A}$, $\mathbf{\Sigma}$, and $\mathbf{\Gamma}$ all become diagonal when they are rotated into the $\mathbf{U}$ and $\mathbf{V}$ coordinates defined by the singular vectors of $\mathbf{F}$. That is, suppose that the rotated matrices $\mathbf{V}^T\mathbf{A}\mathbf{V}$, $\mathbf{U}^T\mathbf{\Sigma}\mathbf{U}$, and $\mathbf{V}^T\mathbf{\Gamma}\mathbf{U}$ are all diagonal. Then the matrices $\mathbf{F}$, $\mathbf{A}$, $\mathbf{\Sigma}$, and $\mathbf{\Gamma}$ can *all* be written in terms of the singular vectors $\mathbf{u}_k$ and $\mathbf{v}_k$ defined by the singular value decomposition of $\mathbf{F}$. That is,

$$\mathbf{F} = \sum_{k=1}^{K} \lambda_k \mathbf{u}_k \mathbf{v}_k^T \quad ,$$

$$\mathbf{A} = \sum_{k=1}^{N} \alpha_k^2 \mathbf{v}_k \mathbf{v}_k^T \quad ,$$

$$\mathbf{\Sigma} = \sum_{k=1}^{M} \sigma_k^2 \mathbf{u}_k \mathbf{u}_k^T \quad , \text{ and}$$

$$\mathbf{\Gamma} = \sum_{k=1}^{K'} \gamma_k \mathbf{v}_k \mathbf{u}_k^T \quad . \tag{52}$$

In other words, these matrices all share the same singular axes; this may be called the case of "coaxial priors." Since $\mathbf{A}$ and $\mathbf{\Sigma}$ are positive definite, $\alpha_k^2 > 0$ for $k = 1, \ldots, N$, and $\sigma_k^2 > 0$ for $k = 1, \ldots, M$. Recall that $K = \mathrm{rk}(\mathbf{F}) \leq K' = \min(M, N)$.

Then the OCLIM filter can be expressed in the same axes as

$$\begin{aligned}
\mathbf{H} &= (\mathbf{A}\mathbf{F}^T + \mathbf{\Gamma})(\mathbf{F}\mathbf{A}\mathbf{F}^T + \mathbf{F}\mathbf{\Gamma} + \mathbf{\Gamma}^T\mathbf{F}^T + \mathbf{\Sigma})^{-1} \\
&= \sum_{k=1}^{K'} \frac{\alpha_k^2 \lambda_k + \gamma_k}{\alpha_k^2 \lambda_k^2 + 2\gamma_k \lambda_k + \sigma_k^2} \mathbf{v}_k \mathbf{u}_k^T \\
&= \sum_{k=1}^{K'} \frac{\alpha_k^2 \lambda_k^2 + \gamma_k \lambda_k}{\alpha_k^2 \lambda_k^2 + 2\gamma_k \lambda_k + \sigma_k^2} \lambda_k^{-1} \mathbf{v}_k \mathbf{u}_k^T \quad ,
\end{aligned} \tag{53}$$

which is exactly the optimal weighted pseudoinverse of $\mathbf{F}$. That is, the optimal weighted pseudoinverse is obtained as a special case of the optimal constrained linear filter when the covariance matrices are coaxial with the response matrix; it is inferior to OCLIM otherwise.

The case of coaxial priors follows naturally from the assumption of uniform priors, so the optimally weighted pseudoinverse yields the minimum mean-square solution for uniform priors. Except for this special case, however, coaxial priors seem unlikely to occur in practice.

The truncated pseudoinverse can also be obtained as a special case, although the assumptions required are rather perverse.

Uniform Priors: The assumption of uniform priors means that $\mathbf{A} = \alpha^2\mathbf{I}$, $\mathbf{\Sigma} = \sigma^2\mathbf{I}$, $\mathbf{\Gamma} = 0$, and all are coaxial with any $\mathbf{F}$. Then the OCLIM filter simplifies to

$$\begin{aligned}
\mathbf{H} &= \mathbf{F}^T(\mathbf{F}\mathbf{F}^T + (\sigma^2/\alpha^2)\mathbf{I})^{-1} \\
&= \sum_{k=1}^{K} \frac{\lambda_k^2}{\lambda_k^2 + \sigma^2/\alpha^2} \lambda_k^{-1} \mathbf{v}_k \mathbf{u}_k^T \quad ,
\end{aligned} \tag{54}$$

where we have used the fact that $\lambda_k = 0$ whenever $k > K$ to reduce the upper limit from K' to K. Since $\mathbf{F}\mathbf{F}^T$ is positive semidefinite, the indicated matrix inverse exists whenever $\sigma^2/\alpha^2 > 0$. The only prior knowledge required is the ratio α^2/σ^2; thus this special case

is useful for noise-tolerant reconstruction given only rough estimates of source and noise amplitude.

This form can be regarded as a Marquardt [34, 35] or Tikhonov [36] regularization of the pseudoinverse $\mathbf{F}^\dagger = \mathbf{F}^T(\mathbf{F}\mathbf{F}^T)^{-1}$. One important difference is that the value of the regularization parameter is determined by the given value of σ^2/α^2 and need not be determined by experiment.

No Prior Information: The case of "no priors" may be approached by letting α^2 go to infinity. In this case, the OCLIM filter goes to the limit

$$\mathbf{H} = \sum_{k=1}^{K} \lambda_k^{-1} \mathbf{v}_k \mathbf{u}_k^T \quad , \tag{55}$$

which is just the Moore-Penrose inverse or the MNLS estimator. Taking the limit as the noise goes to zero ($\sigma^2 \to 0$) yields the same result.

A Posteriori Variance and Confidence Limits

Given the additional assumption that $\mathbf{q}$ and $\mathbf{w}$ are jointly Gaussian, it is possible to determine the a posteriori variance and hence confidence limits on the estimate $\hat{\mathbf{q}}$.

Papoulis gives the following result, which has been restated in matrix form [27]: Suppose that $\mathbf{x}$ and $\mathbf{y}$ are zero-mean, jointly Gaussian random vectors with covariance matrices $\mathbf{\Sigma_{xx}}$ and $\mathbf{\Sigma_{yy}}$ and cross-covariance $\mathbf{\Sigma_{xy}} = \mathbf{\Sigma_{yx}}^T$. Then, for given $\mathbf{y}$, $\mathbf{x}$ is normally distributed with mean

$$\mu_{\mathbf{x}|\mathbf{y}} = \mathbf{\Sigma_{xy}}\mathbf{\Sigma_{yy}}^{-1}\mathbf{y} \tag{56}$$

and variance

$$\mathbf{\Sigma}_{\mathbf{x}|\mathbf{y}} = \mathbf{\Sigma_{xx}} - \mathbf{\Sigma_{xy}}\mathbf{\Sigma_{yy}}^{-1}\mathbf{\Sigma_{yx}} \quad . \tag{57}$$

In the present problem, $\mathbf{b}$ is given and $\mathbf{q}$ is sought. Thus, we evaluate

$$\begin{aligned}
\mathbf{\Sigma_{qq}} &= \mathsf{E}\,\mathbf{q}\mathbf{q}^T = \mathbf{A} \quad ; \\
\mathbf{\Sigma_{qb}} &= \mathsf{E}\,\mathbf{q}(\mathbf{F}\mathbf{q}+\mathbf{w})^T = \mathbf{A}\mathbf{F}^T + \mathbf{\Gamma} \quad ; \quad \text{and} \\
\mathbf{\Sigma_{bb}} &= \mathsf{E}(\mathbf{F}\mathbf{q}+\mathbf{w})(\mathbf{F}\mathbf{q}+\mathbf{w})^T = \mathbf{F}\mathbf{A}\mathbf{F}^T + \mathbf{F}\mathbf{\Gamma} + \mathbf{\Gamma}^T\mathbf{F}^T + \mathbf{\Sigma} \quad .
\end{aligned} \tag{58}$$

Then the mean of $\mathbf{q}$ given $\mathbf{b}$ is

$$\begin{aligned}
\hat{\mathbf{q}} = \mu_{\mathbf{q}|\mathbf{b}} &= \mathbf{\Sigma_{qb}}\mathbf{\Sigma_{bb}}^{-1}\mathbf{b} \\
&= (\mathbf{A}\mathbf{F}^T + \mathbf{\Gamma})(\mathbf{F}\mathbf{A}\mathbf{F}^T + \mathbf{F}\mathbf{\Gamma} + \mathbf{\Gamma}^T\mathbf{F}^T + \mathbf{\Sigma})^{-1}\mathbf{b} \quad ,
\end{aligned} \tag{59}$$

which is exactly the MMSE estimate derived above for $\mathbf{q}$ and $\mathbf{w}$ with arbitrary distributions. Furthermore, the variance of $\mathbf{q}$ given $\mathbf{b}$ is

$$\begin{aligned}
\hat{\mathbf{A}} &= \mathbf{\Sigma}_{\mathbf{q}|\mathbf{b}} \\
&= \mathbf{\Sigma_{qq}} - \mathbf{\Sigma_{qb}}\mathbf{\Sigma_{bb}}^{-1}\mathbf{\Sigma_{bq}} \\
&= \mathbf{A} - (\mathbf{A}\mathbf{F}^T + \mathbf{\Gamma})(\mathbf{F}\mathbf{A}\mathbf{F}^T + \mathbf{F}\mathbf{\Gamma} + \mathbf{\Gamma}^T\mathbf{F}^T + \mathbf{\Sigma})^{-1}(\mathbf{A}\mathbf{F}^T + \mathbf{\Gamma})^T \quad .
\end{aligned} \tag{60}$$

If the noise is uncorrelated with the sources, then $\mathbf{\Gamma} = 0$ and the a posteriori variance becomes

$$\hat{\mathbf{A}} = \mathbf{A} - \mathbf{A}\mathbf{F}^T(\mathbf{F}\mathbf{A}\mathbf{F}^T + \mathbf{\Sigma})^{-1}\mathbf{F}\mathbf{A} \quad . \tag{61}$$

Note that the a posteriori variance does not depend on the actual measurements $\mathbf{b}$ and thus can be computed in advance.

Each diagonal entry $\hat{\alpha}_{nn}^2$ of $\hat{\mathbf{A}}$ is the a posteriori variance of the corresponding estimate q_n; hence each q_n has a standard error equal to $\hat{\alpha}_{nn}$, from which confidence limits can be computed for any desired probability [26].

Furthermore, the a posteriori variance is, by definition,

$$\begin{aligned}\hat{\mathbf{A}} &= \mathsf{E}(\hat{\mathbf{q}} - \mathsf{E}\,\hat{\mathbf{q}})(\hat{\mathbf{q}} - \mathsf{E}\,\hat{\mathbf{q}})^T \\ &= \mathsf{E}(\hat{\mathbf{q}} - \mathbf{q})(\hat{\mathbf{q}} - \mathbf{q})^T\end{aligned}$$

which implies that

$$\mathrm{Tr}(\hat{\mathbf{A}}) = \sum_n \hat{\alpha}_{nn}^2 = \mathsf{E}\,\|\hat{\mathbf{q}} - \mathbf{q}\|^2 = \eta^2 \quad , \tag{62}$$

which is an alternative way to compute η^2.

Computer Implementation

The four reconstruction methods discussed in this paper have been implemented in FORTRAN 77 for noise uncorrelated with sources ($\mathbf{\Gamma} = 0$) and independent priors ($\mathbf{A}$ and $\mathbf{\Sigma}$ diagonal). The LAPACK library [37] was used for linear algebra computations. All computations were done in double precision.

Some tricks were used in the implementation of OCLIM to improve performance; no implementation tricks are known for the other methods. The problem in OCLIM is to compute

$$\hat{\mathbf{q}} = \mathbf{A}\mathbf{F}^T(\mathbf{F}\mathbf{A}\mathbf{F}^T + \mathbf{\Sigma})^{-1}\mathbf{b} \quad , \tag{63}$$

for one or more vectors $\mathbf{b}$, given $\mathbf{F}$, $\mathbf{A}$, and $\mathbf{\Sigma}$. Since $\mathbf{A}$ is diagonal, the expression $\mathbf{F}\mathbf{A}\mathbf{F}^T$ may be written in the simple form

$$\mathbf{F}\mathbf{A}\mathbf{F}^T = \sum_n \alpha_{nn}^2\, \mathbf{f}_n\, \mathbf{f}_n^T \tag{64}$$

where $\mathbf{f}_n$ is the nth column of $\mathbf{F}$. Since $\mathbf{\Sigma}$ is diagonal, adding it to $\mathbf{F}\mathbf{A}\mathbf{F}^T$ requires little additional work.

Nor is it necessary to compute the matrix inverse explicitly. Define $\mathbf{p} = (\mathbf{F}\mathbf{A}\mathbf{F}^T + \mathbf{\Sigma})^{-1}\mathbf{b}$. Then $\mathbf{p}$ can be computed by solving the system $(\mathbf{F}\mathbf{A}\mathbf{F}^T + \mathbf{\Sigma})\mathbf{p} = \mathbf{b}$. Furthermore, $\mathbf{B} = \mathbf{F}\mathbf{A}\mathbf{F}^T + \mathbf{\Sigma}$ is symmetric positive definite and has a Cholesky decomposition $\mathbf{L}\mathbf{L}^T$ with $\mathbf{L}$ lower triangular; using this is more efficient than inverting the matrix or using the LU decomposition [24, 25]. A suitable computational procedure thus proceeds as follows:

1.1 Form the matrix $\mathbf{B} = \mathbf{\Sigma} + \sum_n \alpha_{nn}^2 \mathbf{f}_n \mathbf{f}_n^T$ using $O(M^2 N)$ flops.

1.2 Compute the Cholesky decomposition $\mathbf{L}\mathbf{L}^T$ of $\mathbf{B}$ in $O(M^3)$ flops.

2.1 Solve the system $\mathbf{L}\mathbf{L}^T\mathbf{p} = \mathbf{b}$ using the Cholesky decomposition in $O(M^2)$ flops.

2.2 Compute the solution $\hat{\mathbf{q}} = \mathbf{A}\mathbf{F}^T\mathbf{p}$ in $O(MN)$ flops.

Steps 1.1 and 1.2 do not involve $\mathbf{b}$ and need be done only once for any specified configuration; steps 2.1 and 2.2 must be done for each measurement vector $\mathbf{b}$. Assuming that M and N are of the same order, setup (steps 1.1 and 1.2) costs $O(N^3)$ flops and each estimated source vector costs $O(N^2)$ flops.

It is also useful to compute at least the diagonal of the a posteriori source covariance

$$\begin{aligned}\hat{\mathbf{A}} &= \mathbf{A} - \mathbf{A}\mathbf{F}^T(\mathbf{F}\mathbf{A}\mathbf{F}^T + \mathbf{\Sigma})^{-1}\mathbf{F}\mathbf{A} \\ &= \mathbf{A} - \mathbf{A}\mathbf{F}^T\mathbf{L}^{-T}\mathbf{L}^{-1}\mathbf{F}\mathbf{A} \\ &= \mathbf{A} - (\mathbf{L}^{-1}\mathbf{F}\mathbf{A})^T(\mathbf{L}^{-1}\mathbf{F}\mathbf{A}) \quad . \end{aligned} \tag{65}$$

Let $\mathbf{X} = \mathbf{L}^{-1}\mathbf{F}\mathbf{A}$. Then $\mathbf{L}\mathbf{X} = \mathbf{F}\mathbf{A}$, which may be solved by forward substitution, and $\hat{\mathbf{A}} = \mathbf{A} - \mathbf{X}^T\mathbf{X}$, which may be computed directly. Note that since $\mathbf{A}$ is diagonal, computing $\mathbf{F}\mathbf{A}$ simply requires multiplying each column of $\mathbf{F}$ by the appropriate diagonal entry of $\mathbf{A}$. Thus, a suitable procedure is as follows:

1.3 Form the product $\mathbf{F}\mathbf{A}$ in $O(MN)$ flops.

1.4 Solve $\mathbf{L}\mathbf{X} = \mathbf{F}\mathbf{A}$ by multiplication and forward substitution in $O(M^3)$ flops.

1.5 Compute $\hat{\mathbf{A}} = \mathbf{A} - \mathbf{X}^T\mathbf{X}$ directly in $O(N^3)$ flops.

All of these steps are independent of $\mathbf{b}$ and can be done as part of the setup; the total time required is $O(N^3)$ flops.

Simulation Results and Discussion

The computer implementation just described was used in a Monte Carlo simulation to compare the four inverse methods. All sources were modelled as current dipoles. In the MNLS method, all singular values less than 10^{-10} times the largest singular value were forced to zero.

Three different source configurations were used and are shown in Figures 1, 2, and 3. The same detector configuration was used for all cases and is shown in Figure 4. Each source/detector configuration was tested for five different values of source and noise variance. Theoretical values of the mean reconstruction error η^2, mean residual $\mathsf{E}\,\chi^2$, and mean surprise $\mathsf{E}\,\rho^2$ were computed for each combination of geometry and statistics from the equations given previously. Then ten thousand source distributions were generated, projected, and reconstructed for the same combination. Experimental mean values and

standard errors for η^2, $\mathsf{E}\,\chi^2$, and $\mathsf{E}\,\rho^2$ were computed from the ten thousand test distributions.

In configuration 1, the sources are arranged in a 4×4 cm^2 planar array perpendicular to the detector plane, and centered below that plane with its nearest edge 1 cm away. The source plane contains an 8×8 array of perpendicular current dipoles. The 28 sources in the central cruciform region are assigned a source variance α_A^2; the remaining sources are assigned a (possibly different) source variance α_B^2.

In configuration 2, the sources are arranged in a 5×5 cm^2 planar array parallel to the detector array and centered 3 cm below it. The source array is a 5×5 grid of sources; each source is a pair of dipoles parallel to the sides of the array. This configuration allows each source to take any orientation in the source plane. The 9 sources in the central cruciform region are assigned a source variance α_A^2; the remaining sources are assigned a (possibly different) source variance α_B^2.

In configuration 3, the sources are arranged in a $4 \times 4 \times 4$ cm^3 cube centered 2 cm below the detector array. This cube contains a $4 \times 4 \times 4$ grid of sources, each of which is a pair of dipoles parallel to the detector plane. All sources are assigned the same variance α^2.

All test configurations used the detector array shown in Figure 4. This array has a 12×12 cm^2 planar array of 144 detectors arranged in a 12×12 grid. Each detector measures the magnetic field perpendicular to the plane of the array. Noise amplitudes taken from independent normal distributions with mean zero and variance σ^2 are added to each field measurement.

Table 1 shows the theoretical and experimental results for configuration 1 with uniform priors ($\alpha_A^2 = \alpha_B^2$) at several different signal-to-noise ratios. Note that the theoretical and experimental values all agree within 2 standard errors.

As predicted, OCLIM and OWPIM show identical results for uniform priors. OTPIM typically has slightly larger values of η^2, $\mathsf{E}\,\chi^2$, and $\mathsf{E}\,\rho^2$ than either. MNLS has better $\mathsf{E}\,\chi^2$ values than any of the other methods but its error is orders of magnitude worse. The mean error η^2 and mean residual $\mathsf{E}\,\chi^2$ both increase as the noise increases; the mean surprise $\mathsf{E}\,\rho^2$ decreases.

The knowledge of the approximate source and noise amplitudes provided by the priors has allowed OCLIM, OWPIM, and OTPIM to generate much better solutions than MNLS. That is, even if there is no prior information on the expected source patterns, knowing the expected signal and noise amplitudes regularizes the pseudoinverse and tames an otherwise ill-conditioned problem.

Table 2 shows the theoretical and experimental results for configuration 1 with non-uniform priors ($\alpha_A^2 \neq \alpha_B^2$) at several different signal-to-noise ratios. The theoretical and experimental values again agree within 2 standard errors. Most of the other observations

on Table 1 remain true. The big change is that OCLIM now has a smaller mean error η^2 than any of the other methods. The difference is largest when the noise is small and decreases to insignificance when the noise is large enough.

Computations for configurations 2 and 3 are shown in Tables 3 and 4; the results are similar.

For any of these configurations, the initialization (steps 1.1–1.5) and reconstruction (steps 2.1–2.2) for a hundred data sets take about a second on a workstation class computer. There are only minor differences in the execution time required for the four different reconstruction methods.

The same reconstruction software was used to produce the images shown in figures 5 and 6. Configuration 1 was used with non-uniform priors; specifically, $\alpha_A^2 = 1$, $\alpha_B^2 = 0.01$, and $\sigma^2 = 10^{-16}$. A single source dipole was active with amplitude 8 and all other sources were zero. The lefthand plot of each pair was reconstructed with OCLIM; the righthand plot with OWPIM. The dipole is at the position indicated by the dot and is pointing out of the page. Grey shading indicates areas of current flow into the page.

Figure 5 shows three reconstructions of sources consistent with the priors (that is, sources in region A). The peak produced by OCLIM is consistently higher and narrower than the one produced by OWPIM. For both methods, the peak gets broader and lower as the source gets further from the detector array.

Figure 6 shows two reconstructions of sources inconsistent with the priors. In the first pair, the true source is close to a plausible source and OCLIM maps the true source into a plausible source with substantial artifacts in form of spurious peaks elsewhere. OWPIM finds the true location of the source. In the second pair, the true source is well separated from any plausible source. Both OCLIM and OWPIM find the true source but OCLIM generates several spurious ridges.

Conclusions

If the unknown current distribution is expressed as a linear combination of elementary current distributions in fixed positions, then the magnetic field measurements are linear in the unknown source amplitudes. If, in addition, the cost function to be minimized is either the mean square error (reconstructed minus true currents) or the square residual (measured minus reconstructed fields), then the unknown source amplitudes may be found by solving a linear problem. This offers several advantages: The problem is well understood theroretically and software for its solution is readily available. There is only a single, global minimum. Efficient and reliable computer codes for linear algebra are readily available.

If the sources are localized and statistically uncorrelated, then the prior knowledge of the current distribution can be interpreted as a map of expected power dissipation or current density as a function of position. Conversely, such a map derived from geological

or physiological principles determines the diagonal of the source covariance matrix; the off-diagonal entries are all zero. Correlations between sources, if present, appear as non-zero off-diagonal entries of the covariance matrix.

The minimum-norm least squares (MNLS) method, also known as the Moore-Penrose inverse and the generalized inverse, provides a lower residual than any other method but does not exploit prior knowledge. But if the problem is poorly conditioned and there is measurement noise, its reconstruction error can be orders of magnitude larger than the true current distribution. Magnetic imaging is both noisy and poorly conditioned, so MNLS is not generally suitable.

The weighted pseudoinverse developed by Shim and Cho generalizes MNLS by including an arbitrary weight in each term of the outer product or spectral expansion of the Moore-Penrose inverse; a truncated pseudoinverse is obtained by restricting the weights to zero and one. Choosing the weights to minimize the mean square error yields an optimally weighted pseudoinverse method (OWPIM) or optimally truncated pseudoinverse method (OTPIM); the source and noise covariance matrices determine the optimum but only the diagonal entries are used. Prior knowledge of the source and noise covariance is required but non-uniform priors are permitted only in special cases. OWPIM and OTPIM generally have mean square error larger than OCLIM and residuals larger than MNLS.

The optimal constrained linear inverse method (OCLIM) derived in this paper uses prior knowledge to obtain a minimum mean square error estimate of the current distribution; OCLIM can be efficiently computed using a Cholesky decomposition. Any source and detector configuration is allowed as long as their positions are fixed a priori. Any correlations between source and noise amplitudes are permitted. OCLIM locates point sources more precisely than OWPIM but is prone to artifacts when the true sources are inconsistent with the priors.

OCLIM reduces to the optimally weighted pseudoinverse method when the source amplitudes are independent and identically distributed and to the minimum-norm least squares estimate in the limit of no measurement noise or no prior knowledge of the source amplitudes.

All four methods are fast to compute, taking about a second on a workstation for a problem with 64 sources and 144 detectors.

Of these methods, OCLIM appears the best suited to magnetic imaging, since it exploits prior information, provides the minimum reconstruction error, and is no more expensive to compute than the others.

Acknowledgements

I am grateful to Prof. Thomas F. Budinger for suggesting the problem of using prior information in magnetic source imaging and to Dr. James G. Berryman to pointing out the connections to Marquardt regularization and iterative nonlinear reconstruction algorithms.

References

[1] Riitta Hari and Risto J. Ilmoniemi. Cerebral magnetic fields. *CRC Crit. Rev. Biomed. Eng.*, 14(2):93–126, 1986.

[2] Jukka Sarvas. Basic mathematical and electromagnetic concepts of the biomagnetic inverse problem. *Phys. Med. Biol.*, 32(1):11–22, 1987.

[3] Susumu Sato, Marshall Balish, and Robert Muratore. Principles of magnetoencephalography. *J. Clin. Neurophysiol.*, 8(2):144–156, April 1991.

[4] A. van Oosterom. History and evolution of methods for solving the inverse problem. *J. Clin. Neurophysiol.*, 8(4):371–380, October 1991.

[5] Gerhard Stroink. Cardiomagnetic imaging. In Barry L. Zaret, Leon Kaufman, Alan S. Berson, and Rosalie A. Dunn, editors, *Frontiers in Cardiovascular Imaging*, chapter 11, pages 161–177. Raven Press, New York, 1993.

[6] J. S. Kallman and J. G. Berryman. Weighted least-squares criteria for electrical impedance tomography. *IEEE Trans. Med. Imaging*, 11(2):284–292, June 1992.

[7] J. G. Berryman and R. V. Kohn. Variational constraints for electrical impedance tomography. *Phys. Rev. Lett.*, 65(3):325–328, 16 July 1990.

[8] B[ernd] Lütkenhöner, K. Lehnertz, M. Hoke, and C. Pantev. On the biomagnetic inverse problem in the case of multiple dipoles. *Acta Oto-Laryngologica*, Suppl 491:94–105, 1991.

[9] Manbir Singh, R. Richardo Brechner, and Victor W. Henderson. Neuromagnetic localization using magnetic resonance images. *IEEE Trans. Med. Imaging*, MI–11(1):129–134, March 1992.

[10] M. Singh, D. Doria, V. W. Henderson, G. C. Huth, and J. Beatty. Reconstruction of images from neuro-magnetic fields. *IEEE Trans. Nuclear Sci.*, NS–31(1):585–589, 1984.

[11] Brian Jeffs, Richard Leahy, and Manbir Singh. An evaluation of methods for neuromagnetic image reconstruction. *IEEE Trans. Biomed. Eng.*, BME–34(9):713–723, September 1987.

[12] Jia-Zhu Wang, Samuel J. Williamson, and Lloyd Kaufman. Magnetic source images determined by a lead-field analysis: The unique minimum-norm least-squares estimation. *IEEE Trans. Biomed. Eng.*, BME–39(7):665–675, July 1992.

[13] Jia-Zhu Wang. Minimum-norm least-squares estimation: Magnetic source images for a spherical model head. *IEEE Trans. Biomed. Eng.*, BME–40(4):387–396, April 1993.

[14] Ceon Ramon, Michael G. Meyer, Alan C. Nelson, Francis A. Spelman, and Jeff Lamping. Simulation studies of biomagnetic computed tomography. *IEEE Trans. Biomed. Eng.*, BME–40(4):317–322, April 1993.

[15] L. A. Shepp and Y. Vardi. Maximum likelihood reconstruction for emission tomography. *IEEE Trans. Med. Imaging*, MI-1(2):113ff, October 1982.

[16] Y. S. Shim and Z. H. Cho. SVD pseudoinversion image reconstruction. *IEEE Trans. ASSP*, ASSP-29(4):904–909, August 1981.

[17] Carl W. Helstrom. Image restoration by the method of least squares. *J. Opt. Soc. Am.*, 57(3):297–303, 1967.

[18] Warren E. Smith, William J. Dallas, Walter H. Kullman, and Heidi A. Schlitt. Linear estimation theory applied to the reconstruction of a 3-D vector current distribution. *Appl. Opt.*, 29(5):658–667, February 1990.

[19] Seho Oh, Ceon Ramon, Robert J. Marks II, Alan C. Nelson, and Michael G. Meyer. Resolution enhancement of biomagnetic images using the method of alternating projections. *IEEE Trans. Biomed. Eng.*, BME–40(4):323–328, April 1993.

[20] Christine E. Miller and Craig S. Henriquez. Finite element analysis of bioelectric phenomena. *CRC Crit. Rev. Biomed. Eng.*, 18(3):207–33, 1990.

[21] M. Thevenet, O. Bertrand, F. Perrin, T. Dumont, and J. Pernier. The finite element method for a realistic head model of electrical brain activities: Preliminary results. *Clin. Phys. Physiol. Meas.*, 12(Suppl A):89–94, 1991.

[22] A. van Oosterom. Mathematical aspects of source modeling. *Acta Oto-Laryngologica*, Suppl 491:70–79, 1991.

[23] John D. Kraus. *Electromagnetics.* McGraw-Hill Book Company, Inc., third edition, 1984.

[24] Gene H. Golub and Charles F. Van Loan. *Matrix Computations.* Johns Hopkins Unversity Press, second edition, 1989.

[25] David S. Watkins. *Fundamentals of Matrix Computations.* John Wiley & Sons, 1991.

[26] Paul G. Hoel, Sidney C. Port, and Charles J. Stone. *Introduction to Statistical Theory.* Houghton Mifflin Company, 1971.

[27] Athanasios Papoulis. *Probability, Random Variables, and Stochastic Processes.* McGraw-Hill, third edition, 1991.

[28] E. H. Moore. On the reciprocal of the general algebraic matrix. *Bull. Am. Math. Soc.*, 26:389 and 394–395, 1920.

[29] R. Penrose. A generalized inverse for matrices. *Proc. Cambridge Philos. Soc.*, 51:406–413, 1955.

[30] S. L. Campbell and C. D. Meyer, Jr. *Generalized Inverses of Linear Transformations.* Dover Publications, Inc., 1991.

[31] Harry C. Andrews and B[obby] R[ay] Hunt. *Digital Image Restoration.* Prentice-Hall, Inc., 1977.

[32] Thomas F. Budinger, Grant T. Gullberg, and Ronald H. Huesman. Emission computed tomography. In Gabor T. Herman, editor, *Image Reconstruction from Projections*, volume 32 of *Topics in Applied Physics*, chapter 5, pages 147–246. Springer-Verlag, 1979.

[33] Avinash C. Kak and Malcolm Slaney. *Principles of Computerized Tomographic Imaging.* IEEE Press, 1988.

[34] Donald W. Marquardt. An algorithm for least-squares estimation of nonlinear parameters. *J. Soc. Indust. Appl. Math.*, 11(2):431–441, June 1963.

[35] Donald W. Marquardt. Generalized inverses, ridge regression, biased linear estimation, and nonlinear estimation. *Technometrics*, 12(3):591–612, August 1970.

[36] Andrei Nikolaevich Tikhonov and Vasiliy Y. Arsenin. *Solutions of Ill-posed Problems.* Halsted Press, 1977.

[37] E. Anderson, Z. Bai, C. Bischof, J. Demmel, J. Dongarra, J. Du Croz, A. Greenbaum, S. Hammarling, A. McKenney, S. Ostrouchov, and D. Sorenson. *LAPACK Users' Guide.* Society for Industrial and Applied Mathematics, Philadelphia, 1992.

Appendix A

Assumption A states that that none of the source amplitudes q_n or the noise amplitudes w_m is almost surely equal to a linear combination of the remaining source and noise amplitudes. That is, every source and noise amplitude has some non-zero residual variance even after the effect of every other source and noise amplitude has been accounted for. This appendix derives certain useful consequences of that assumption.

Definition: A set of random vectors $\mathbf{x}_1, \ldots, \mathbf{x}_n$ is linearly dependent if there exist constant vectors $\mathbf{u}_1, \ldots, \mathbf{u}_n$, not all zero, such that $\mathbf{u}_1^T\mathbf{x}_1 + \cdots + \mathbf{u}_n^T\mathbf{x}_n = 0$ almost surely. If the set $\mathbf{x}_1, \ldots, \mathbf{x}_n$ is not linearly dependent, it is linearly independent.

Proposition: Assumption A implies that the set $\{\mathbf{q}, \mathbf{w}\}$ is linearly independent.

Proof: Suppose that $\mathbf{q}$ and $\mathbf{w}$ are linearly dependent. Then there exist vectors $\mathbf{u}$ and $\mathbf{v}$, not both zero, such that $\mathbf{u}^T\mathbf{q} + \mathbf{v}^T\mathbf{w} = \sum_i u_i q_i + \sum_j v_j w_j = 0$ almost surely. But at least one component of $\mathbf{u}$ or $\mathbf{v}$ is non-zero. Say that component is u_i. Then solving for q_i yields an linear expression in the remaining components that is almost surely equal to q_i. Thus assumption A must be false.

Proposition: Suppose that a set of random vectors is linearly dependent. Then adding any additional random vector to the set yields a linearly dependent set.

Proof: Set the coefficient of the added vector to zero.

Corollary: Any subset of a linearly independent set is linearly independent.

Corollary: The vector $\mathbf{q}$ is linearly independent. So is $\mathbf{w}$.

Proposition: The measurement vector $\mathbf{b} = \mathbf{F}\mathbf{q} + \mathbf{w}$ is linearly independent.

Proof: Suppose that $\mathbf{b}$ is linearly dependent. Then there exists a non-zero constant $\mathbf{u}$ such that $\mathbf{u}^T\mathbf{b} = 0$ almost surely. But this implies that $\mathbf{u}^T\mathbf{F}\mathbf{q} + \mathbf{u}^T\mathbf{w} = 0$ almost surely. Thus $\mathbf{q}$ and $\mathbf{w}$ must be linearly dependent.

Proposition: Suppose that the random vector $\mathbf{x}$ is linearly independent. Then the correlation matrix $\mathbf{\Sigma_x} = \mathsf{E}\,\mathbf{x}\mathbf{x}^T$ is nonsingular.

Proof: Suppose that $\mathbf{\Sigma_x}$ is singular. Then there exists a constant $\mathbf{u} \neq 0$ such that $\mathbf{u}^T\mathbf{\Sigma_x}\mathbf{u} = 0$. But $\mathbf{u}^T\mathbf{\Sigma_x}\mathbf{u} = \mathbf{u}^T\,\mathsf{E}(\mathbf{x}\mathbf{x}^T)\mathbf{u} = \mathsf{E}(\mathbf{u}^T\mathbf{x}\mathbf{x}^T\mathbf{u}) = \mathsf{E}\,\|\mathbf{u}^T\mathbf{x}\|^2$ which can be zero only if $\mathbf{u}^T\mathbf{x} = 0$ almost surely. But this implies that $\mathbf{x}$ is linearly dependent.

Corollary: The covariance matrices $\mathbf{A} = \mathsf{E}\,\mathbf{q}\mathbf{q}^T$, $\mathbf{\Sigma} = \mathsf{E}\,\mathbf{w}\mathbf{w}^T$, and $\mathbf{B} = \mathsf{E}\,\mathbf{b}\mathbf{b}^T$ are all invertible.

Corollary: Since all covariance matrices are symmetric and positive semidefinite, $\mathbf{A}$, $\mathbf{\Sigma}$, and $\mathbf{B}$ are symmetric positive definite and have Cholesky decompositions in the forms

$$\mathbf{A} = \mathbf{R}\mathbf{R}^T, \qquad \mathbf{\Sigma} = \mathbf{S}\mathbf{S}^T, \quad \text{and} \qquad \mathbf{B} = \mathbf{L}\mathbf{L}^T \tag{66}$$

where $\mathbf{R}$, $\mathbf{S}$, and $\mathbf{L}$ are all lower triangular and invertible.

Proposition: If $\mathbf{x}$ is linearly independent, then $\mathsf{E}\,||\mathbf{D}\mathbf{x}||^2 > 0$ for every matrix $\mathbf{D} \neq 0$.

Proof: Suppose that $\mathsf{E}\,||\mathbf{D}\mathbf{x}||^2 = 0$. Then, almost surely, $||\mathbf{D}\mathbf{x}|| = 0$, which implies that $\mathbf{D}\mathbf{x} = 0$, which implies that $\mathbf{x}$ is linearly dependent.

Table 1. This table shows how the reconstruction quality varies with noise level when the four different methods are used on configuration 1 with uniform priors.

		OCLIM	OWPIM	OTPIM	MNLS
Configuration 1 with $\sigma^2 = 1.000 \times 10^{-20}$, $\alpha_A^2 = 1.000$, $\alpha_B^2 = 1.000$, $SNR = 254.9$ db, and 10000 data sets:					
η^2	theo	18.193	18.194	19.543	2.417×10^5
	expr	18.157 ± 0.059	18.157 ± 0.059	19.533 ± 0.062	$(2.391 \pm 0.021) \times 10^5$
$\mathsf{E}\,\chi^2$	theo	98.187	98.191	99.144	84.999
	expr	98.012 ± 0.140	98.006 ± 0.140	98.986 ± 0.143	84.797 ± 0.130
$\mathsf{E}\,\rho^2$	theo	45.807	45.806	47.543	2.417×10^5
	expr	45.919 ± 0.094	45.918 ± 0.094	47.636 ± 0.099	$(2.391 \pm 0.021) \times 10^5$
Configuration 1 with $\sigma^2 = 1.000 \times 10^{-16}$, $\alpha_A^2 = 1.000$, $\alpha_B^2 = 1.000$, $SNR = 174.9$ db, and 10000 data sets:					
η^2	theo	30.762	30.762	31.860	2.417×10^9
	expr	30.729 ± 0.077	30.729 ± 0.077	31.862 ± 0.079	$(2.391 \pm 0.021) \times 10^9$
$\mathsf{E}\,\chi^2$	theo	110.762	110.762	112.324	85.000
	expr	110.666 ± 0.148	110.666 ± 0.148	112.254 ± 0.151	84.797 ± 0.130
$\mathsf{E}\,\rho^2$	theo	33.238	33.238	33.860	2.417×10^9
	expr	33.352 ± 0.080	33.352 ± 0.080	33.983 ± 0.083	$(2.391 \pm 0.021) \times 10^9$
Configuration 1 with $\sigma^2 = 1.000 \times 10^{-12}$, $\alpha_A^2 = 1.000$, $\alpha_B^2 = 1.000$, $SNR = 94.9$ db, and 10000 data sets:					
η^2	theo	43.890	43.890	45.452	2.417×10^{13}
	expr	43.918 ± 0.092	43.918 ± 0.092	45.503 ± 0.094	$(2.391 \pm 0.021) \times 10^{13}$
$\mathsf{E}\,\chi^2$	theo	123.890	123.890	125.658	85.000
	expr	123.730 ± 0.157	123.730 ± 0.157	125.476 ± 0.160	84.797 ± 0.130
$\mathsf{E}\,\rho^2$	theo	20.110	20.110	21.452	2.417×10^{13}
	expr	20.135 ± 0.061	20.135 ± 0.061	21.454 ± 0.069	$(2.391 \pm 0.021) \times 10^{13}$
Configuration 1 with $\sigma^2 = 1.000 \times 10^{-8}$, $\alpha_A^2 = 1.000$, $\alpha_B^2 = 1.000$, $SNR = 14.9$ db, and 10000 data sets:					
η^2	theo	56.880	56.880	57.803	2.417×10^{17}
	expr	56.878 ± 0.105	56.878 ± 0.105	57.824 ± 0.107	$(2.391 \pm 0.021) \times 10^{17}$
$\mathsf{E}\,\chi^2$	theo	136.880	136.880	137.989	85.000
	expr	136.667 ± 0.165	136.667 ± 0.165	137.739 ± 0.167	84.797 ± 0.130
$\mathsf{E}\,\rho^2$	theo	7.120	7.120	7.803	2.417×10^{17}
	expr	7.161 ± 0.035	7.161 ± 0.035	7.883 ± 0.043	$(2.391 \pm 0.021) \times 10^{17}$
Configuration 1 with $\sigma^2 = 1.000 \times 10^{-4}$, $\alpha_A^2 = 1.000$, $\alpha_B^2 = 1.000$, $SNR = -65.1$ db, and 10000 data sets:					
η^2	theo	63.923	63.923	64.000	2.417×10^{21}
	expr	63.995 ± 0.113	63.995 ± 0.113	64.068 ± 0.113	$(2.391 \pm 0.021) \times 10^{21}$
$\mathsf{E}\,\chi^2$	theo	143.923	143.923	144.080	85.000
	expr	143.651 ± 0.170	143.651 ± 0.170	143.806 ± 0.170	84.797 ± 0.130
$\mathsf{E}\,\rho^2$	theo	0.077	0.077	0.000	2.417×10^{21}
	expr	0.076 ± 0.001	0.076 ± 0.001	0.000 ± 0.000	$(2.391 \pm 0.021) \times 10^{21}$

Table 2. This table shows how the reconstruction quality varies with noise level when the four different methods are used on configuration 1 with non-uniform priors.

		OCLIM	OWPIM	OTPIM	MNLS
Configuration 1 with $\sigma^2 = 1.000 \times 10^{-20}$, $\alpha_A^2 = 1.000$, $\alpha_B^2 = 0.010$, $SNR = 245.8$ db, and 10000 data sets:					
η^2	theo	4.486	10.727	11.419	2.417×10^5
	expr	4.456 ± 0.025	10.709 ± 0.041	11.400 ± 0.043	$(2.391 \pm 0.021) \times 10^5$
$\mathsf{E}\chi^2$	theo	101.352	98.999	100.316	84.999
	expr	101.172 ± 0.141	98.809 ± 0.140	100.117 ± 0.143	84.797 ± 0.130
$\mathsf{E}\rho^2$	theo	42.651	231.248	256.449	8.441×10^6
	expr	42.763 ± 0.090	232.159 ± 0.821	257.459 ± 0.943	$(8.395 \pm 0.081) \times 10^6$
Configuration 1 with $\sigma^2 = 1.000 \times 10^{-16}$, $\alpha_A^2 = 1.000$, $\alpha_B^2 = 0.010$, $SNR = 165.8$ db, and 10000 data sets:					
η^2	theo	10.209	17.039	17.519	2.417×10^9
	expr	10.205 ± 0.041	17.002 ± 0.054	17.492 ± 0.055	$(2.391 \pm 0.021) \times 10^9$
$\mathsf{E}\chi^2$	theo	114.253	111.774	111.585	85.000
	expr	114.161 ± 0.150	111.688 ± 0.149	111.483 ± 0.150	84.797 ± 0.130
$\mathsf{E}\rho^2$	theo	29.747	225.663	257.338	8.443×10^{10}
	expr	29.747 ± 0.075	225.201 ± 0.775	257.600 ± 0.927	$(8.395 \pm 0.081) \times 10^{10}$
Configuration 1 with $\sigma^2 = 1.000 \times 10^{-12}$, $\alpha_A^2 = 1.000$, $\alpha_B^2 = 0.010$, $SNR = 85.8$ db, and 10000 data sets:					
η^2	theo	17.366	22.307	22.939	2.417×10^{13}
	expr	17.403 ± 0.057	22.313 ± 0.064	22.936 ± 0.065	$(2.391 \pm 0.021) \times 10^{13}$
$\mathsf{E}\chi^2$	theo	128.069	125.447	126.082	85.000
	expr	127.872 ± 0.159	125.267 ± 0.158	125.880 ± 0.160	84.797 ± 0.130
$\mathsf{E}\rho^2$	theo	15.931	169.524	211.813	8.443×10^{14}
	expr	15.905 ± 0.053	168.929 ± 0.697	211.027 ± 0.971	$(8.395 \pm 0.081) \times 10^{14}$
Configuration 1 with $\sigma^2 = 1.000 \times 10^{-8}$, $\alpha_A^2 = 1.000$, $\alpha_B^2 = 0.010$, $SNR = 5.8$ db, and 10000 data sets:					
η^2	theo	24.393	26.655	27.093	2.417×10^{17}
	expr	24.404 ± 0.069	26.644 ± 0.072	27.089 ± 0.073	$(2.391 \pm 0.021) \times 10^{17}$
$\mathsf{E}\chi^2$	theo	139.623	138.394	141.165	85.000
	expr	139.386 ± 0.167	138.158 ± 0.166	140.937 ± 0.170	84.797 ± 0.130
$\mathsf{E}\rho^2$	theo	4.377	74.427	88.174	8.443×10^{18}
	expr	4.327 ± 0.027	73.841 ± 0.430	87.658 ± 0.622	$(8.395 \pm 0.081) \times 10^{18}$
Configuration 1 with $\sigma^2 = 1.000 \times 10^{-4}$, $\alpha_A^2 = 1.000$, $\alpha_B^2 = 0.010$, $SNR = -74.2$ db, and 10000 data sets:					
η^2	theo	28.333	28.349	28.360	2.417×10^{21}
	expr	28.303 ± 0.075	28.320 ± 0.075	28.331 ± 0.075	$(2.391 \pm 0.021) \times 10^{21}$
$\mathsf{E}\chi^2$	theo	143.973	143.973	144.028	85.000
	expr	143.704 ± 0.170	143.705 ± 0.170	143.760 ± 0.170	84.797 ± 0.130
$\mathsf{E}\rho^2$	theo	0.027	0.653	0.000	8.443×10^{22}
	expr	0.027 ± 0.000	0.649 ± 0.008	0.000 ± 0.000	$(8.395 \pm 0.081) \times 10^{22}$

Table 3. This table shows how the reconstruction quality varies with noise level when the four different methods are used on configuration 2 with non-uniform priors.

		OCLIM	OWPIM	OTPIM	MNLS
Configuration 2 with $\sigma^2 = 1.000 \times 10^{-20}$, $\alpha_A^2 = 1.000$, $\alpha_B^2 = 0.010$, $SNR = 265.9$ db, and 10000 data sets:					
η^2	theo	2.158	6.040	6.040	6.040×10^0
	expr	2.141 ± 0.020	6.024 ± 0.029	6.024 ± 0.029	$(6.024 \pm 0.029) \times 10^0$
$\mathsf{E}\,\chi^2$	theo	103.884	104.010	104.010	104.010
	expr	104.010 ± 0.145	103.987 ± 0.145	103.987 ± 0.145	103.987 ± 0.145
$\mathsf{E}\,\rho^2$	theo	40.000	236.020	236.020	2.360×10^2
	expr	39.930 ± 0.090	235.748 ± 1.024	235.748 ± 1.024	$(2.357 \pm 0.010) \times 10^2$
Configuration 2 with $\sigma^2 = 1.000 \times 10^{-16}$, $\alpha_A^2 = 1.000$, $\alpha_B^2 = 0.010$, $SNR = 185.9$ db, and 10000 data sets:					
η^2	theo	2.164	6.046	6.046	6.046×10^0
	expr	2.147 ± 0.020	6.031 ± 0.029	6.031 ± 0.029	$(6.031 \pm 0.029) \times 10^0$
$\mathsf{E}\,\chi^2$	theo	104.271	104.033	104.000	104.000
	expr	104.258 ± 0.145	104.020 ± 0.145	103.987 ± 0.145	103.987 ± 0.145
$\mathsf{E}\,\rho^2$	theo	39.729	236.254	236.326	2.363×10^2
	expr	39.656 ± 0.089	235.975 ± 1.025	236.048 ± 1.025	$(2.360 \pm 0.010) \times 10^2$
Configuration 2 with $\sigma^2 = 1.000 \times 10^{-12}$, $\alpha_A^2 = 1.000$, $\alpha_B^2 = 0.010$, $SNR = 105.9$ db, and 10000 data sets:					
η^2	theo	2.495	7.765	8.106	7.084×10^1
	expr	2.478 ± 0.020	7.731 ± 0.031	8.070 ± 0.032	$(7.037 \pm 0.062) \times 10^1$
$\mathsf{E}\,\chi^2$	theo	114.023	110.680	109.840	104.000
	expr	113.974 ± 0.151	110.665 ± 0.149	109.834 ± 0.150	103.987 ± 0.145
$\mathsf{E}\,\rho^2$	theo	29.977	281.677	306.829	3.298×10^3
	expr	29.890 ± 0.076	280.733 ± 1.087	305.460 ± 1.173	$(3.282 \pm 0.028) \times 10^3$
Configuration 2 with $\sigma^2 = 1.000 \times 10^{-8}$, $\alpha_A^2 = 1.000$, $\alpha_B^2 = 0.010$, $SNR = 25.9$ db, and 10000 data sets:					
η^2	theo	7.460	12.532	13.433	6.480×10^5
	expr	7.434 ± 0.034	12.494 ± 0.044	13.374 ± 0.047	$(6.435 \pm 0.062) \times 10^5$
$\mathsf{E}\,\chi^2$	theo	129.024	126.412	129.758	104.000
	expr	128.948 ± 0.159	126.333 ± 0.158	129.683 ± 0.164	103.987 ± 0.145
$\mathsf{E}\,\rho^2$	theo	14.976	186.464	207.953	3.062×10^7
	expr	14.928 ± 0.050	186.283 ± 0.775	207.488 ± 1.001	$(3.047 \pm 0.028) \times 10^7$
Configuration 2 with $\sigma^2 = 1.000 \times 10^{-4}$, $\alpha_A^2 = 1.000$, $\alpha_B^2 = 0.010$, $SNR = -54.1$ db, and 10000 data sets:					
η^2	theo	18.065	18.219	18.320	6.480×10^9
	expr	17.965 ± 0.059	18.117 ± 0.059	18.215 ± 0.059	$(6.435 \pm 0.062) \times 10^9$
$\mathsf{E}\,\chi^2$	theo	143.737	143.729	144.285	104.000
	expr	143.679 ± 0.169	143.668 ± 0.169	144.224 ± 0.169	103.987 ± 0.145
$\mathsf{E}\,\rho^2$	theo	0.263	5.804	0.000	3.062×10^{11}
	expr	0.262 ± 0.002	5.834 ± 0.042	0.000 ± 0.000	$(3.047 \pm 0.028) \times 10^{11}$

Table 4. This table shows how the reconstruction quality varies with noise level when the four different methods are used on configuration 3 with uniform priors.

		OCLIM	OWPIM	OTPIM	MNLS
Configuration 3 with $\sigma^2 = 1.000 \times 10^{-20}$, $\alpha^2 = 1.000$, $SNR = 251.0$ db, and 10000 data sets:					
η^2	theo	26.490	26.499	28.702	9.029×10^5
	expr	26.471 ± 0.069	26.471 ± 0.069	28.680 ± 0.074	$(9.140 \pm 0.071) \times 10^5$
$\mathsf{E}\chi^2$	theo	42.533	42.483	42.017	20.997
	expr	42.414 ± 0.089	42.431 ± 0.089	41.951 ± 0.093	20.939 ± 0.065
$\mathsf{E}\rho^2$	theo	101.510	101.491	106.684	9.014×10^5
	expr	101.304 ± 0.140	101.284 ± 0.140	106.510 ± 0.149	$(9.141 \pm 0.071) \times 10^5$
Configuration 3 with $\sigma^2 = 1.000 \times 10^{-16}$, $\alpha^2 = 1.000$, $SNR = 171.0$ db, and 10000 data sets:					
η^2	theo	54.663	54.663	57.426	9.029×10^9
	expr	54.655 ± 0.102	54.655 ± 0.102	57.386 ± 0.106	$(9.140 \pm 0.071) \times 10^9$
$\mathsf{E}\chi^2$	theo	70.663	70.662	72.235	21.000
	expr	70.540 ± 0.116	70.540 ± 0.116	72.050 ± 0.123	20.939 ± 0.065
$\mathsf{E}\rho^2$	theo	73.337	73.337	77.426	9.029×10^9
	expr	73.100 ± 0.119	73.100 ± 0.119	77.242 ± 0.129	$(9.140 \pm 0.071) \times 10^9$
Configuration 3 with $\sigma^2 = 1.000 \times 10^{-12}$, $\alpha^2 = 1.000$, $SNR = 91.0$ db, and 10000 data sets:					
η^2	theo	86.192	86.192	89.808	9.029×10^{13}
	expr	86.165 ± 0.128	86.165 ± 0.128	89.745 ± 0.132	$(9.140 \pm 0.071) \times 10^{13}$
$\mathsf{E}\chi^2$	theo	102.192	102.192	105.511	21.000
	expr	102.047 ± 0.139	102.047 ± 0.139	105.360 ± 0.147	20.939 ± 0.065
$\mathsf{E}\rho^2$	theo	41.808	41.808	45.808	9.029×10^{13}
	expr	41.632 ± 0.087	41.632 ± 0.087	45.619 ± 0.101	$(9.140 \pm 0.071) \times 10^{13}$
Configuration 3 with $\sigma^2 = 1.000 \times 10^{-8}$, $\alpha^2 = 1.000$, $SNR = 11.0$ db, and 10000 data sets:					
η^2	theo	117.197	117.197	119.933	9.029×10^{17}
	expr	117.049 ± 0.151	117.049 ± 0.151	119.771 ± 0.154	$(9.140 \pm 0.071) \times 10^{17}$
$\mathsf{E}\chi^2$	theo	133.197	133.197	137.076	21.000
	expr	133.137 ± 0.160	133.137 ± 0.160	137.034 ± 0.167	20.939 ± 0.065
$\mathsf{E}\rho^2$	theo	10.803	10.803	11.933	9.029×10^{17}
	expr	10.760 ± 0.040	10.760 ± 0.040	11.859 ± 0.054	$(9.140 \pm 0.071) \times 10^{17}$
Configuration 3 with $\sigma^2 = 1.000 \times 10^{-4}$, $\alpha^2 = 1.000$, $SNR = -69.0$ db, and 10000 data sets:					
η^2	theo	127.950	127.950	128.000	9.029×10^{21}
	expr	127.710 ± 0.159	127.710 ± 0.159	127.760 ± 0.159	$(9.140 \pm 0.071) \times 10^{21}$
$\mathsf{E}\chi^2$	theo	143.950	143.950	144.051	21.000
	expr	143.904 ± 0.168	143.904 ± 0.168	144.004 ± 0.168	20.939 ± 0.065
$\mathsf{E}\rho^2$	theo	0.050	0.050	0.000	9.029×10^{21}
	expr	0.050 ± 0.000	0.050 ± 0.000	0.000 ± 0.000	$(9.140 \pm 0.071) \times 10^{21}$

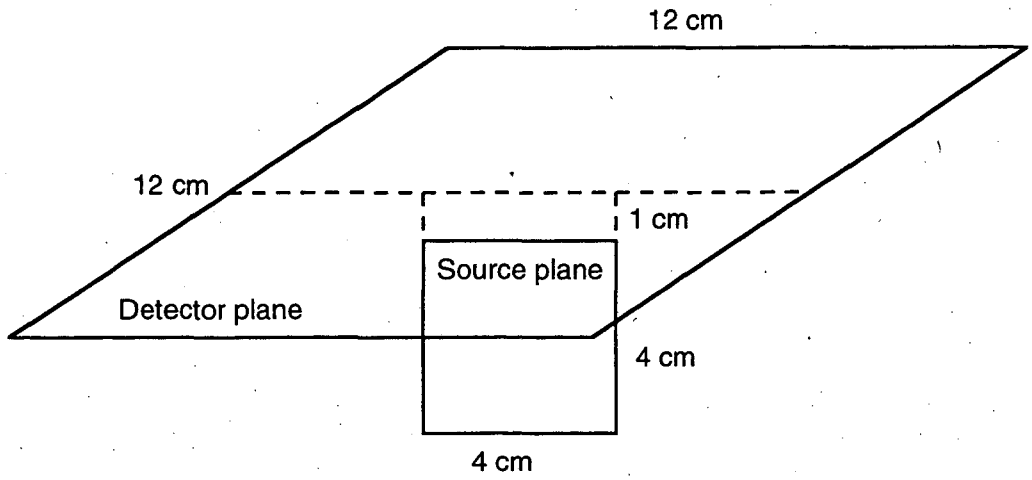

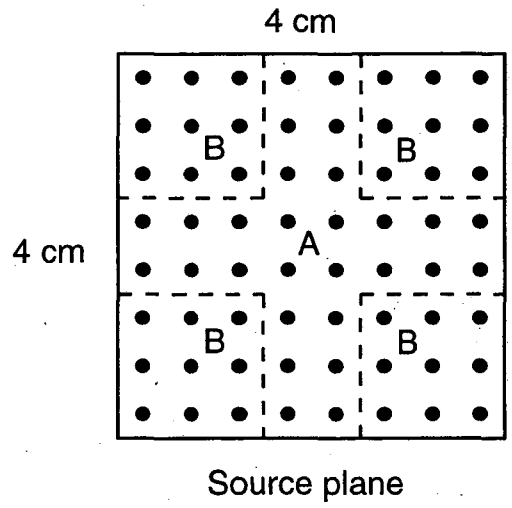

Figure 1. Test configuration 1. The source plane is perpendicular to the detector plane and contains 64 dipoles perpendicular to the source plane. The dipoles in region A have higher expected power.

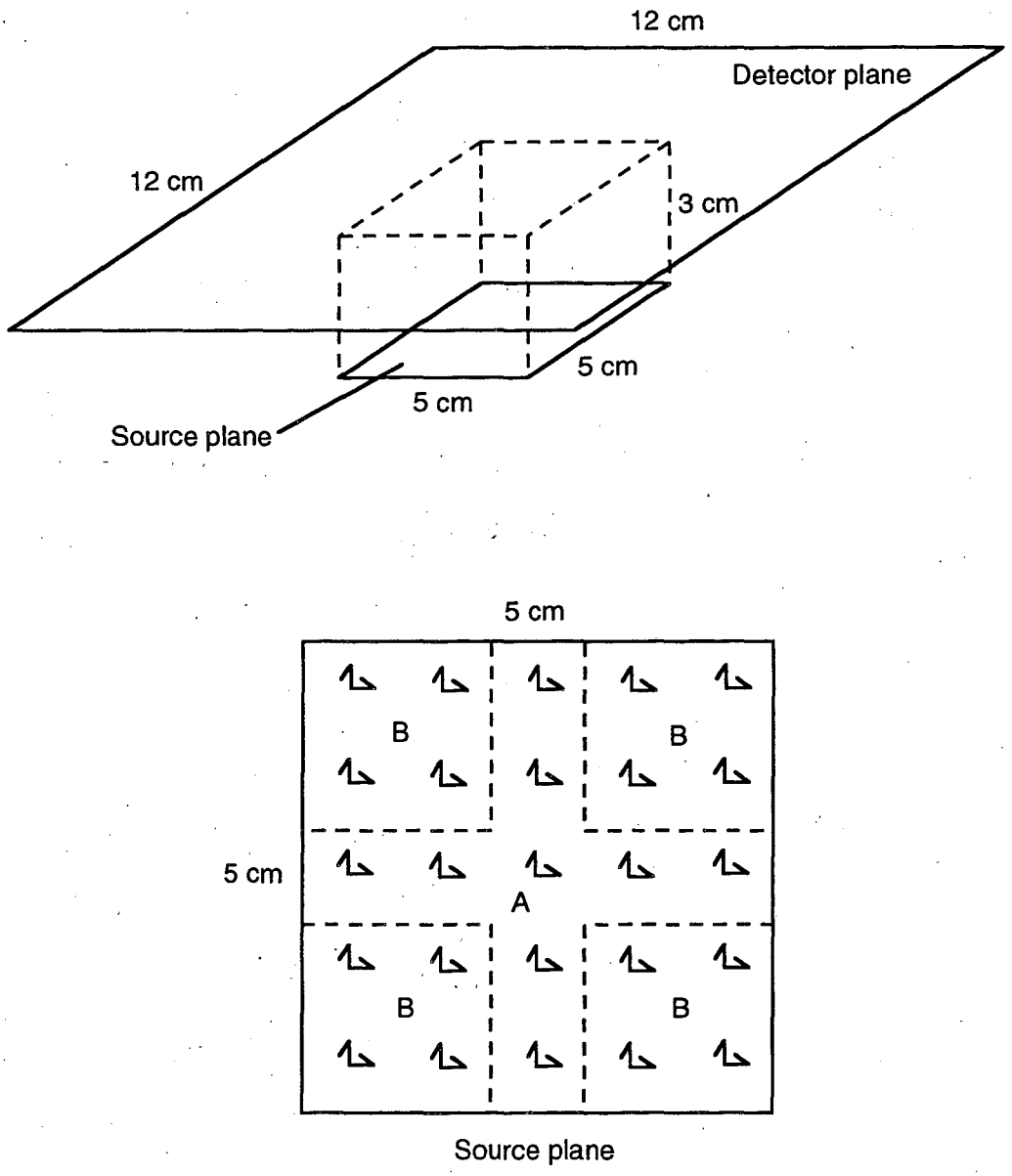

Figure 2. Test configuration 2. The source plane is parallel to the detector plane and contains 25 dipole pairs parallel to the detector plane. Dipoles in region A have higher expected power.

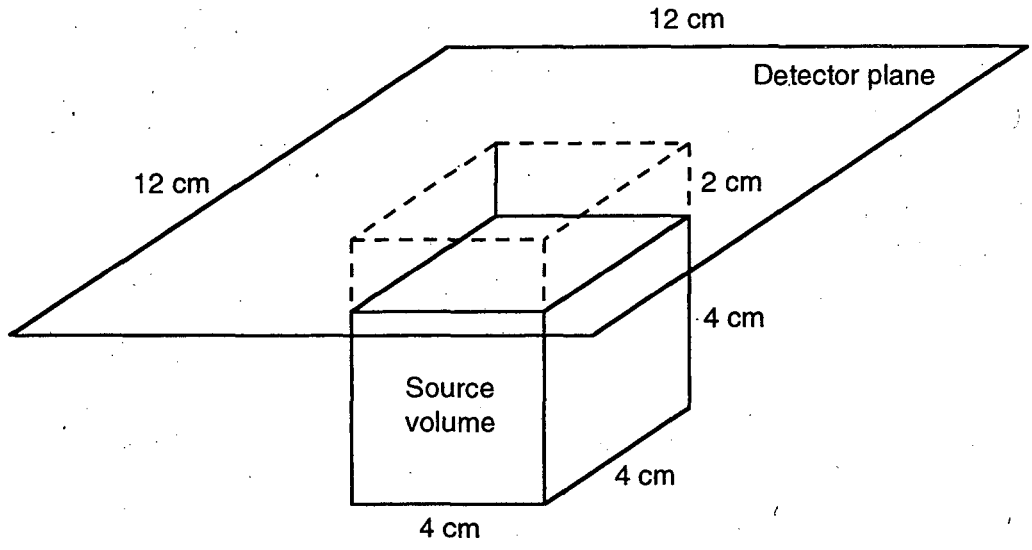

Figure 3. Test configuration 3. The source volume contains a cubical grid of 64 dipole pairs parallel to the detector plane. All dipoles have the same expected power.

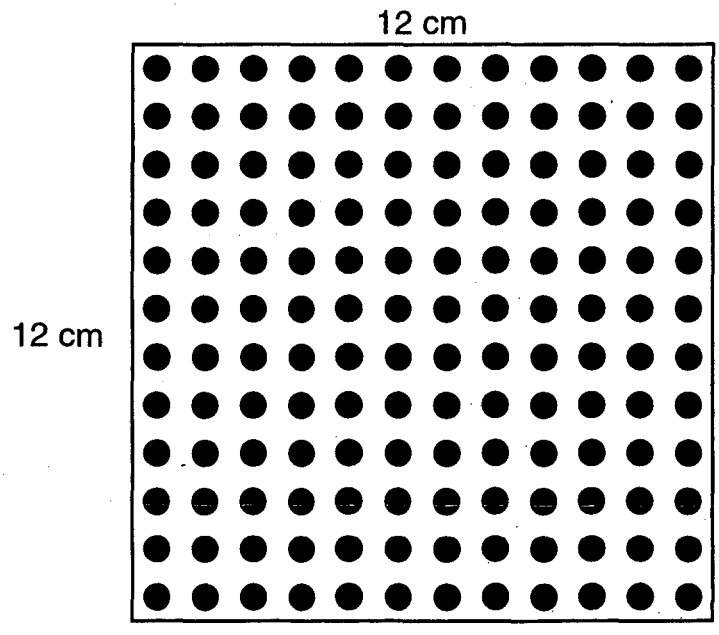

Figure 4. The detector grid contains a 12 by 12 array of sensors that sample the field perpendicular to the array.

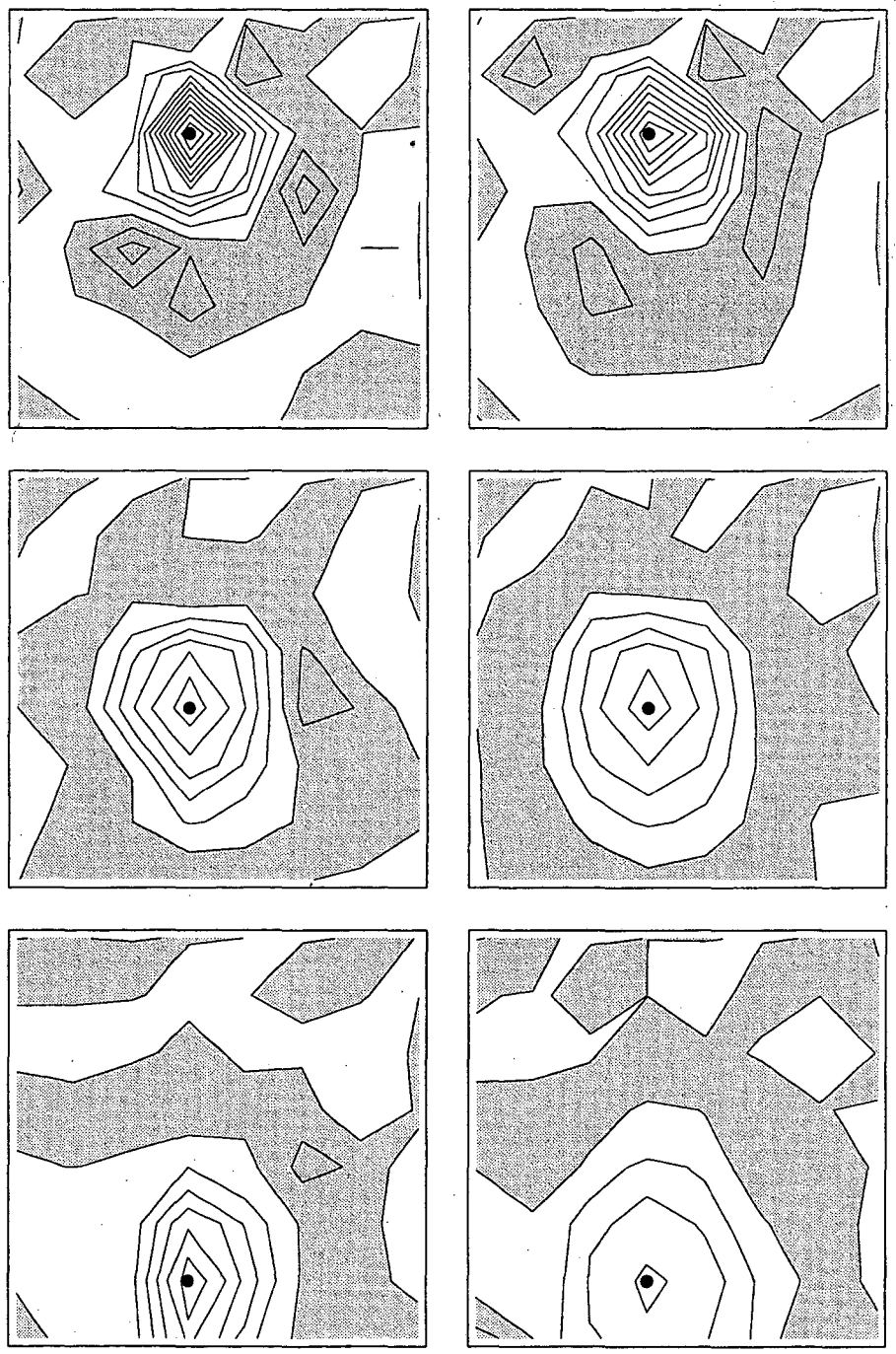

Figure 5. Reconstruction of sources consistent with the prior knowledge. The lefthand image of each pair shows the reconstruction using OCLIM with prior information; the righthand image shows the reconstruction using OWPIM with uniform priors. The true distribution is a single dipole out of the page at the position indicated by the dot. Grey shading indicates areas of current flow into the page.

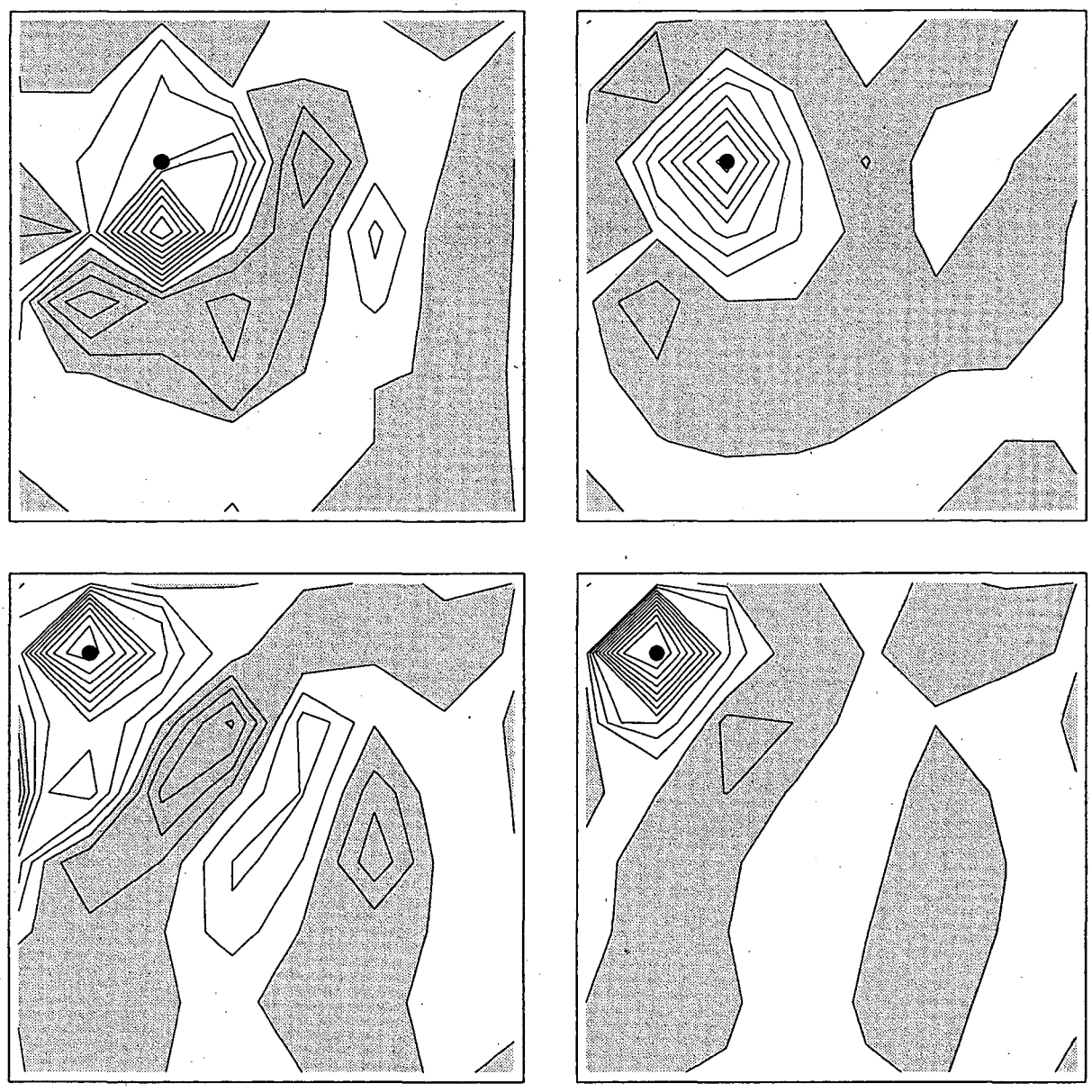

Figure 6. Reconstruction of sources inconsistent with the prior knowledge. The lefthand image of each pair shows the reconstruction using OCLIM with prior information; the righthand image shows the reconstruction with uniform priors. The true distribution is a single dipole out of the page at the position indicated by the dot. Grey shading indicates areas of current flow into the page.

LAWRENCE BERKELEY LABORATORY
UNIVERSITY OF CALIFORNIA
TECHNICAL INFORMATION DEPARTMENT
BERKELEY, CALIFORNIA 94720

ABH482
LBL Libraries